Investigation of the contribution of transporters to the pharmacokinetics of drugs targeted to liver and the effect of their genetic polymorphisms in humans
（肝指向性薬物のヒトの体内動態支配因子としてのトランスポーターの寄与および遺伝子多型による機能変動の解析）

前田　和哉

Contents

Abbreviations

ABC	ATP-binding cassette
ACE	angiotensin converting enzyme
ANOVA	analysis of variance
ASBT	apical sodium-dependent bile salt transporter
AST	aspartate aminotransferase
AUC	area under the plasma concentration-time curve
BCRP	breast cancer resistance protein
BSEP	bile salt export pump
CYP	cytochrome P450
EHBR	Eisai hyperbilirubinemic rat
ES	embryonic stem
GST	glutathione-S-transferase
GUDC	glycoursodeoxycholate
HMG-CoA	3-hydroxymethylglutaryl coenzyme A
LCA	lithocholate
MDR	multidrug resistance
mEH	microsomal epoxide hydrorase
MRP	multidrug resistance associated protein
NTCP	Na^+-taurocholate co-transporting polypeptide
OAT	organic anion transporter
OATP	organic anion transporting polypeptide
OCT	organic cation transporter
OST	organic solute transporter
PET	positron emission tomography
RAF	relative activity factor
siRNA	small interference RNA
SLC	solute carrier
SNP	single nucleotide polymorphism
SPECT	single photon emission computed tomography
SULT	sulfo-transferase
TCA	taurocholate
TUDC	tauroursodeoxycholate
UDCA	ursodeoxycholate
UGT	UDP-glucuronosyl transferase

General Introduction

The liver is one of the most important organs for the detoxification of endogenous and exogenous compounds. In the process of detoxification, compounds are first taken up into the liver, then metabolized by Phase I enzymes, such as cytochrome P450 (CYP), which mainly catalyze the oxidation of a variety of sub-structures, and Phase II conjugation enzymes, such as glutathione-S-transferase (GST), UDP-glucuronosyl transferase (UGT) and sulfo-transferase (SULT), which add hydrophilic groups to the compounds and/or their metabolites, which are then excreted into the bile. In general, the membrane permeability is thought to be largely determined by the molecular weight and Log P value (water/octanol partition coefficient)(Levin, 1980). However, some recent reports have indicated that hydrophilic compounds which cannot easily penetrate the plasma membrane because of their physicochemical properties are efficiently taken up into specific organs, such as liver and kidney(Mizuno et al., 2003). Currently, many uptake and efflux transporters have been identified and characterized in human liver and in some cases they play an important role in drug disposition. For example, pravastatin, an HMG-CoA reductase inhibitor, is efficiently taken up by the liver, which is a

pharmacological target of this drug and retained in the hepatobiliary system for a long time by enterohepatic circulation with only minimal systemic exposure, which results in an increase in its pharmacological effects and a reduction in its side effects, such as rhabdomyolysis. Several reports have demonstrated that the beneficial pharmacokinetic properties of pravastatin are achieved by several uptake and efflux transporters, such as organic anion transporting polypeptide (OATP) 1B1 and multidrug resistance associated protein (MRP) 2 in the liver and, possibly, the small intestine(Tamai et al., 1995; Yamazaki et al., 1996; Hsiang et al., 1999; Nakai et al., 2001; Sasaki et al., 2002; Nozawa et al., 2004). Several SLC (solute carrier) family uptake transporters are expressed on the sinusoidal membrane of the human liver (Fig. G-1)(Hagenbuch and Meier, 1996; Muller and Jansen, 1997; Hagenbuch and Meier, 2003). Na^+-taurocholate co-transporting polypeptide (NTCP) is responsible for the transport of bile acids in a Na+-dependent manner(Hagenbuch and Meier, 1994). Organic anion transporter (OAT) 2 is involved in the uptake of small hydrophilic organic anions(Sun et al., 2001), while organic cation transporter (OCT) 1 plays a role in the uptake of small organic cations(Zhang et al., 1997). OATP family transporters can accept several kinds of bulky organic anions(Hagenbuch and

Meier, 2003). Several ABC (ATP-binding cassette) transporters, which can pump out the compounds from cells by using the energy of ATP hydrolysis, are located on the bile canalicular membrane (Fig. G-1). MRP2 is thought to be responsible for the biliary excretion of glucuronides, glutathione-conjugates and some unconjugated organic anions(Suzuki and Sugiyama, 1998; Konig et al., 1999). Bile salt export pump (BSEP) is important for the efflux of bile acids(Noe et al., 2001; Byrne et al., 2002; Noe et al., 2002). Multidrug resistance (MDR) 1 (P-glycoprotein) is involved in the efflux of various kinds of hydrophobic neutral and cationic compounds(Tanigawara, 2000; Varadi et al., 2002). Breast cancer resistance protein (BCRP) has been cloned most recently and can also accept several kinds of compound, especially sulfate conjugates(Suzuki et al., 2003). The main characteristic of molecules involved in the detoxification of xenobiotics, such as metabolic enzymes and transporters, is their broad substrate specificity and molecular diversity, which is advantageous for the elimination of many kinds of structurally-diverse compounds.

Based on the pharmacokinetic concept explained above, the apparent intrinsic clearance ($CL_{uint,all}$) can be explained by the following equation (Fig. G-2)(Shitara et al., 2005).

$$CL_{u\,\mathrm{int},all} = CL_{\mathrm{inf}} \times \frac{CL_{metab} + CL_{seq}}{(CL_{metab} + CL_{seq}) + CL_{eff}} \qquad \text{(Eq. G-1)}$$

, where CL_{inf}, CL_{metab}, CL_{eff}, CL_{seq} represent the intrinsic clearance for hepatic uptake, metabolism, backflux from cell to blood and efflux from cell to bile, respectively. If the sum of CL_{metab} and CL_{seq} is much greater than CL_{eff}, Eq. G-1 can be described as Eq. G-2.

$$CL_{u\,\mathrm{int},all} = CL_{\mathrm{inf}} \qquad \text{(Eq. G-2)}$$

In this case, the rate-determining process of the overall intrinsic clearance is hepatic uptake. On the other hand, if the sum of CL_{metab} and CL_{seq} is much smaller than CL_{eff}, Eq. G-1 can be described as Eq. G-3.

$$CL_{u\,\mathrm{int},all} = CL_{\mathrm{inf}} \times \frac{CL_{metab} + CL_{seq}}{CL_{eff}} \qquad \text{(Eq. G-3)}$$

We should note that intrinsic hepatic clearance is always proportional to the uptake clearance (CL_{inf}) regardless of the situation. Therefore, a change in the uptake clearance has a direct influence on the intrinsic hepatic clearance. Especially for the uptake of organic anions in human liver, OATP1B1 and OATP1B3 are thought to be important because they are almost exclusively expressed in liver and accept a wide variety of organic anions including endogenous compounds, such as bilirubin and thyroxine, and

clinically-important drugs, such as rifampicin, HMG-CoA reductase inhibitors (so called "statins"), ACE inhibitors and angiotensin II receptor antagonists(Hagenbuch and Meier, 2003). Due to the high homology of these molecules, the substrate specificities generally overlap each other and one compound can be transported by both transporters. To predict the effect of the functional change in each transporter caused by genetic polymorphisms and transporter-mediated drug interactions on the overall pharmacokinetics of drugs, it is essential to have information about the contribution of each transporter to the overall membrane transport process. Fortunately, we can now use cryopreserved human hepatocytes for the characterization of uptake activity in human liver. Shitara et al. have demonstrated that the transport activity of typical transporter substrates (estradiol-17β-glucuronide, taurocholate) in cryopreserved human hepatocytes is almost fully retained compared with that in freshly isolated hepatocytes(Shitara et al., 2003b) and using human hepatocytes, it has been shown that the drug-drug interaction between cyclosporin A and cerivastatin is mainly caused by inhibition of the hepatic uptake of cerivastatin by cyclosporin A(Shitara et al., 2003a). We recently established the three methods to estimate the contribution of OATP1B1, 1B3 and 2B1 to the overall

hepatic uptake of organic anions: (1) Using transporter-selective substrates as reference compounds, we can calculate the ratio of the uptake clearance in human hepatocytes to that in transporter expression systems and then estimate the uptake clearance mediated by a specific transporter by multiplying that ratio by the uptake clearance of the test compounds in expression system. This method (called RAF (relative activity factor) method) was originally used in the field of CYP enzymes and we have applied this method to the field of hepatic uptake transporters. (2) Using Western blot analysis, we can estimate the ratio of the band density of a specific transporter in human hepatocytes to that in the expression system and carry out the calculation using the same concept as that described earlier. (3) Using transporter-selective inhibitors, we can estimate the inhibitable portion of the transporter-specific uptake in the presence of selective inhibitors in human hepatocytes(Hirano et al., 2004; Hirano et al., 2006; Ishiguro et al., 2006). From our analyses, we have shown that the relative contribution of OATP1B1 and OATP1B3 depends on the individual compounds even in the same category of drugs(Ishiguro et al., 2006; Yamashiro et al., 2006).

Therefore, to further investigate the importance of each uptake transporter

for the hepatic clearance of drugs, in Part I we investigated the role of uptake transporters in the hepatic uptake of ursodeoxycholate (UDCA) by using human cryopreserved hepatocytes and transporter expression systems. UDCA is often used for the treatment of several hepatic diseases. Like substrates for anion transporters, UDCA undergoes enterohepatic circulation being efficiently taken up into liver, excreted into bile and reabsorbed from the intestine. However, although the pharmacological target of UDCA is liver, its transport mechanism has not yet been fully characterized.

Then, to demonstrate the importance of the function of the uptake transporter in the clinical pharmacokinetics of drugs, in Part II, we performed a clinical study to investigate the effect of the haplotype of OATP1B1 on the pharmacokinetics of pravastatin, valsartan and temocapril. Nishizato et al. have clearly demonstrated that the area under the plasma concentration-time curve (AUC) of pravastatin in subjects with OATP1B1*15 (Asn130Asp & Val174Ala) is significantly greater than that in non-carriers of the *15 allele, which shows that the OATP1B1*15 mutant results in a reduction in the hepatic clearance of pravastatin(Nishizato et al., 2003). However, at that time, there were few reports about the change in the pharmacokinetics of the substrate

drugs for OATP1B1 other than statins.

Through *in vitro* and *in vivo* clinical studies, I wish to show the importance of hepatic uptake transporters in the pharmacokinetics of several drugs which selectively accumulate in the liver.

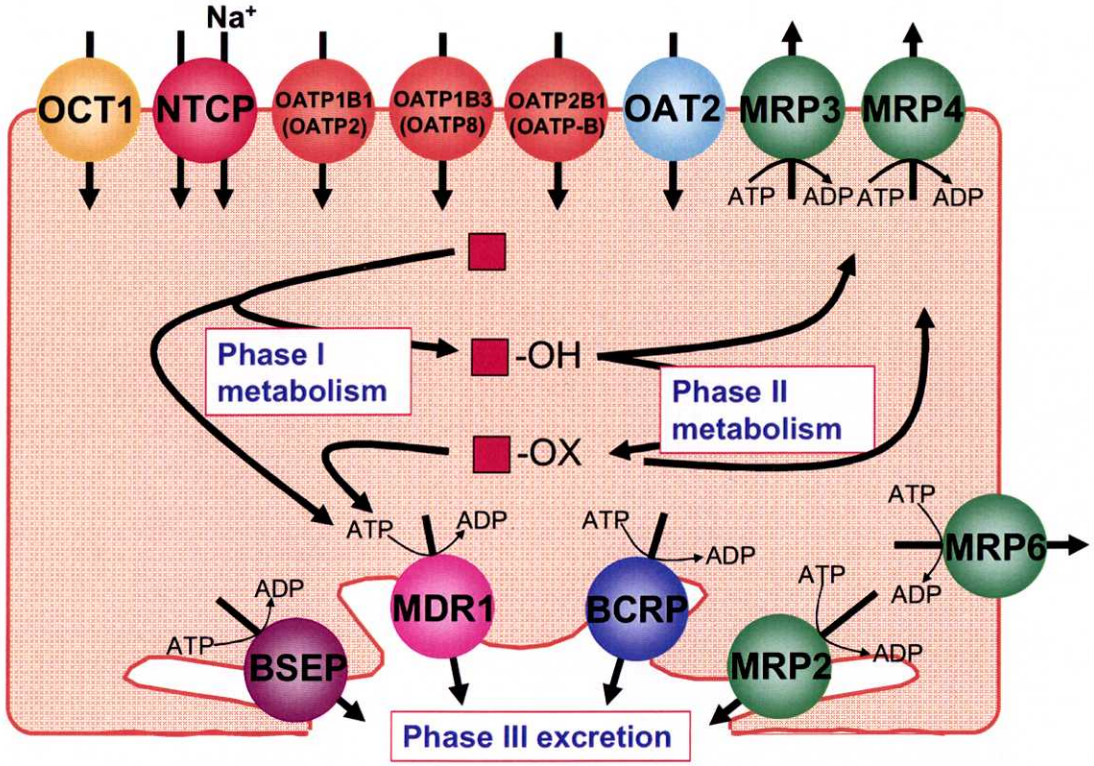

Fig. G-1 Schematic diagram of the detoxification system in human liver

OCT: organic cation transporter
OAT: organic anion transporter
OATP: organic anion transporting polypeptide
NTCP: Na^+-taurocholate cotransporting polypeptide
MRP: multidrug resistance associated protein
MDR: multidrug resistance
BSEP: bile salt export pump
BCRP: breast cancer resistance protein

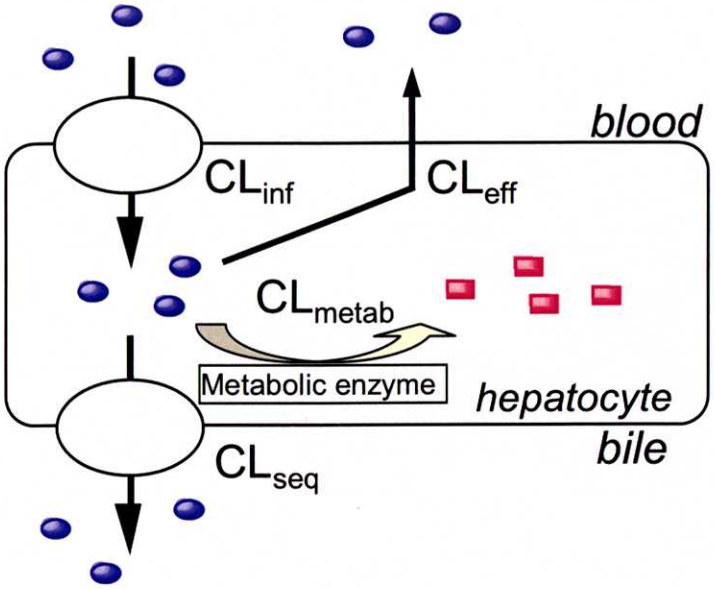

Fig. G-2 Detailed mechanisms for the clearance of drugs in liver

CL_{inf}: intrinsic uptake clearance from blood to cells
CL_{eff}: intrinsic backflux clearance from cells to blood
CL_{metab}: intrinsic metabolic clearance
CL_{seq}: intrinsic efflux clearance from cells to bile

Part I

Uptake of ursodeoxycholate and its conjugates by human hepatocytes: role of Na^+-taurocholate cotransporting polypeptide (NTCP), organic anion transporting polypeptide (OATP) 1B1 (OATP-C) and OATP1B3 (OATP8).

Abstract

Ursodeoxycholate (UDCA) is widely used for the treatment of cholestatic liver disease. After oral administration, UDCA is absorbed, taken up efficiently by hepatocytes, and conjugated mainly with glycine to form glycolursodeoxy-cholate (GUDC) or partly with taurine to form tauroursodeoxycholate (TUDC), which undergo enterohepatic circulation. In this study, to check whether three basolateral transporters – Na^+-taurocholate cotransporting polypeptide (NTCP, SLC10A1), organic anion transporting polypeptide (OATP) 1B1 (OATP-C) and OATP1B3 (OATP8) mediate uptake of UDC, GUDC, and TUDC by human hepatocytes, we investigated their transport properties using transporter-expressing HEK293 cells and human cryopreserved hepatocytes. TUDC and GUDC could be taken up via human NTCP, OATP1B1 and OATP1B3, whereas UDCA could be transported significantly by NTCP, but not OATP1B1 and OATP1B3 in our expression systems. We observed a time-dependent and saturable uptake of UDCA and its conjugates by human cryopreserved hepatocytes and more than half of the overall uptake involved a saturable component. Kinetic analyses revealed that the contribution of Na^+-dependent and -independent pathways to the uptake of UDCA or TUDC was very similar,

while the Na^+-independent uptake of GUDC was predominant. These results suggest that UDCA and its conjugates are taken up by both multiple saturable transport systems and non-saturable transport in human liver with different contributions. These results provide an explanation for the efficient hepatic clearance of UDCA and its conjugates in patients receiving UDCA therapy.

Introduction

Ursodeoxycholate (UDCA) is a natural, non-cytotoxic bile acid that is used as a drug for the treatment of various cholestatic disorders(Hofmann, 1999; Paumgartner and Beuers, 2002), though the exact molecular mechanisms of its pharmacological actions have not been clarified(Paumgartner and Beuers, 2002)(Fig. I-1A). Under normal conditions, UDCA accounts for only about 3 % of the total bile acids in human bile. However, the fraction of UDCA conjugates in total bile acids increases up to 30-50 % in patients receiving UDCA(Invernizzi et al., 1999). Lindor et al. reported that after repetitive administration of UDCA for 2 years to primary biliary cirrhosis patients, the percentage of UDCA in serum bile acids is well correlated with that in biliary bile acids, but in some patients plasma bile acids were enriched with UDCA, but not biliary bile acids(Lindor et al., 1998). They also reported that changes in biliary UDCA concentration, rather than in serum concentration, correlated well with the decrease in the concentration of alkaline phosphatase, aspartate aminotransferase (AST) and bilirubin in the serum, which are clinical markers of hepatic function(Lindor et al., 1998). Therefore, in order to predict the effectiveness of the treatment for individual patients, it is important to understand the molecular mechanism of

UDCA accumulation in the bile.

After oral administration of UDCA, it is absorbed from the small intestine, efficiently extracted by hepatocytes and conjugated mainly with glycine to give glycoursodeoxycholate (GUDC) and partly with taurine, to give tauroursodeoxycholate (TUDC). GUDC and TUDC are secreted into bile and join endogenous bile acids circulating enterohepatically. So hepatic uptake process of UDCA and its conjugates partly contributes to their long-time retention in bile (Fig. I-1B).

Traditionally, the hepatic uptake of bile acids consists of Na^+-independent and Na^+-dependent pathways(Van Dyke et al., 1982). For example, cholate is taken up into isolated rat hepatocytes mainly in an Na^+-independent manner, while about 80 % of the taurocholate uptake is mediated by the Na^+-dependent route(Anwer and Hegner, 1978). At the present time, it is known that Na^+-taurocholate cotransporting polypeptide (NTCP) is involved in Na^+-dependent uptake(Hagenbuch and Meier, 1994), whereas the organic anion transporting polypeptide (OATP) family, also present on the basolateral membrane, is responsible for Na^+-independent uptake(Hagenbuch and Meier, 2003). OATP1B1 (OATP-C) and OATP1B3

(OATP8) are expressed exclusively in the liver and transport a wide variety of endogenous compounds as well as drugs(Hagenbuch and Meier, 2003). They can also transport not only unconjugated bile acids (e.g. cholate) but also conjugated bile acids (e.g. glycocholate and taurocholate)(Hagenbuch and Meier, 2003). Regarding the uptake mechanism of UDCA and its conjugates in humans, it has been reported that TUDC can be a substrate of NTCP and OATP1A2 (OATP-A)(Kullak-Ublick et al., 1995; Meier et al., 1997), although the role of OATP1A2 in its hepatic uptake is thought to be minor because the expression level of OATP1A2 in human liver is very low(Alcorn et al., 2002). On the other hand, some previous reports have shown that TUDC can be transported by rat Ntcp, Oatp1a1 (Oatp1)(Eckhardt et al., 1999), Oatp1a4 (Oatp2)(Reichel et al., 1999) and Oatp1a5 (Oatp3)(Walters et al., 2000), and GUDC can be transported by Oatp1a5 in rats(Walters et al., 2000). Which transporters, if any, mediate the transport of UDCA has not been clarified. Poupon et al. used perfused rat liver to demonstrate that UDCA can be taken up in a saturable manner, which indicates the involvement of transporters in the hepatic uptake of UDCA(Poupon et al., 1988). Because there is no strict one-to-one relationship between rodent Oatps and human OATPs and the

composition of conjugated bile acids in bile differs markedly between rats and humans, it seemed to be important for us to perform transport analyses of UDCA and its conjugates using human gene products and human hepatocytes. In this study, we have characterized the transport of UDCA, GUDC and TUDC by NTCP, OATP1B1 and OATP1B3 using transporter expression systems and human cryopreserved hepatocytes.

Materials & Methods

Materials

[^{3}H]Ursodeoxycholate (20 Ci/mmol) was obtained from SibTech Inc. (Newington, CT) by customized synthesis. 22,23-[^{3}H]Tauroursodeoxycholate (10 Ci/mmol) and 22,23-[^{3}H]glycoursodeoxycholate (11 Ci/mmol) were synthesized by reductive tritiation of the unsaturated precursor. (see Ref. (Sorscher et al., 1992)). [^{3}H]Taurocholate (2 Ci/mmol) was purchased from PerkinElmer Life Sciences (Boston, MA). Unlabeled sodium ursodeoxycholate, sodium tauroursodeoxycholate and sodium glycoursodeoxycholate were kindly provided by Mitsubishi Pharma Co. (Osaka, Japan). Unlabeled taurocholate was purchased from Sigma Chemical Co. (St. Louis, MO). All other chemicals used were commercially available and of reagent grade.

Construction of human NTCP-expressing cells

The human NTCP cDNA was amplified by PCR using human liver cDNA purchased from BD Biosciences Clontech (Palo Alto, CA) as a template. The sequences of the forward and reverse primer to obtain the full-length NTCP cDNA were 5'-GCTAGCATCGATGCCGCCATGGAGGCCCACAACGCGTC-3'

and 5'-AAGCTTGCGGCCGCCTAGGCTGTGCAAGGGGAGC-3'. The amplified cDNA fragment was TA-cloned into the pGEM vector (Promega, CA, USA). Then, human NTCP-cloned vector was digested with Nhe I and Hind III and subcloned into pcDNA3.1(+)(Invitrogen, Carlsbad, CA). HEK293 cells were transfected with expression vector using FuGENE6 (Roche Diagnostics Corp., Indianapolis, IN), according to the manufacturer's instruction. After G418 selection (800 μg/mL) for 3 weeks, single colonies were screened using the transport activity of taurocholate and the clone with the highest activity was maintained and used for further analyses.

Cell Culture

Transporter-expressing HEK293 cells and vector-control cells were grown in Dulbecco's modified Eagle's medium (low glucose version) (Invitrogen, Carlsbad, CA) supplemented with 10 % fetal bovine serum, 100 units/mL penicillin, 100 μg/mL streptomycin at 37 °C with 5 % CO_2 and 95 % humidity.

Transport Assay in transporter expression systems

The transport study was carried out as described previously(Hirano et al.,

2004). Cells were seeded in 12-well plates at a density of 1.5×10^5 cells/well. Cell culture medium was replaced with culture medium supplemented with 5 mM sodium-butyrate 24 h before transport assay to induce the expression of OATP1B1, OATP1B3 and OAT2. Uptake was initiated by adding Krebs-Henseleit buffer containing radiolabeled and unlabeled substrates after cells had been washed twice and preincubated with Krebs-Henseleit buffer at 37°C for 15 min. To measure the Na^+-independent uptake, sodium chloride and sodium bicarbonate in Krebs-Henseleit buffer were replaced with choline chloride and choline bicarbonate. The Krebs-Henseleit buffer consists of 118 mM NaCl, 23 mM $NaHCO_3$, 4.8 mM KCl, 1.0 mM KH_2PO_4, 1.20 mM $MgSO_4$, 12.5 mM HEPES, 5 mM glucose, and 1.53 mM $CaCl_2$ adjusted to pH 7.4. The uptake was terminated at a designated time by adding ice-cold Krebs-Henseleit buffer after removal of the incubation buffer. Then, cells were washed twice with 1 mL ice-cold Krebs-Henseleit buffer, solubilized in 500 μL 0.2 N NaOH, and kept overnight at 4°C. Aliquots (500 μL) were transferred to scintillation vials after adding 250 μL 0.4 N HCl. The radioactivity associated with the cells and incubation buffer was measured in a liquid scintillation counter (LS6000SE; Beckman Coulter, Inc.) after adding 2 mL scintillation fluid (Clear-sol I, NACALAI

TESQUE, Kyoto, Japan) to the scintillation vials. The remaining 50 μL of the aliquots of cell lysate was used to determine the protein concentration by the method of Lowry with bovine serum albumin as a standard.

Transport by human cryopreserved hepatocytes

This experiment was performed as described previously(Shitara et al., 2003b). Cryopreserved human hepatocytes were purchased from In Vitro Technologies (Baltimore, USA). Just before the study, the hepatocytes (1 mL suspension) were thawed at 37 °C, then immediately suspended in 10 mL ice-cold Krebs-Henseleit buffer and centrifuged (50 *g*) for 2 min at 4 °C, followed by removal of the supernatant. This procedure was repeated once more to remove cryopreservation buffer and then cells were resuspended in the same buffer to give a cell density of 1.0×10^6 viable cells/mL for the uptake study. The number of viable cells was determined by trypan blue staining. The average fraction of viable cells in human cryopreserved hepatocytes was 65-80%. To measure the uptake in the absence of Na^+, sodium chloride and sodium bicarbonate in Krebs-Henseleit buffer were replaced with choline chloride and choline bicarbonate. Prior to the uptake studies, the cell suspensions were

prewarmed in an incubator at 37 °C for 3 min. The uptake studies were initiated by adding an equal volume of buffer containing labeled and unlabeled substrates to the cell suspension. After incubation at 37 °C for 0.5, 2 or 5 min, the reaction was terminated by separating the cells from the substrate solution. For this purpose, an aliquot of 80 µL incubation mixture was collected and placed in a centrifuge tube (450 µL) containing 50 µL 2 N NaOH under a layer of 100 µL of oil (density, 1.015, a mixture of silicone oil and mineral oil; Sigma-Aldrich, St. Louis, MO), and subsequently, the sample tube was centrifuged for 10 s using a tabletop centrifuge (10,000*g*; Beckman Microfuge E; Beckman Coulter, Inc., Fullerton, CA). During this process, hepatocytes passed through the oil layer into the alkaline solution. After an overnight incubation in alkali to dissolve the hepatocytes, the centrifuge tube was cut and each compartment was transferred to a scintillation vial. The compartment containing the dissolved cells was neutralized with 50 µL 2 N HCl, mixed with scintillation cocktail, and the radioactivity was measured in a liquid scintillation counter.

Data Analyses

The uptake was expressed as the uptake volume (µL/mg protein), given as the

amount of radioactivity associated with the cells (dpm/mg protein) divided by its concentration in the incubation medium (dpm/μL). To estimate the hepatic clearance of the substrate in human hepatocytes, uptake clearance ($CL_{(2\ min\text{-}0.5\ min)}$ (μL/min/10^6 cells)) was calculated by subtracting the uptake volume (V_d (μL/10^6 cells)) at 0.5 min from that at 2 min as shown in (Eq. I-1), because the uptake at the Y-intercept (time 0) of the graph is thought to represent non-specific adsorption to the culture dish or the cell surface of the hepatocytes and 0.5 min is the shortest measurable sampling point from a practical point of view. Also, the saturable hepatic clearance (CL_{hep} (μL/min/10^6 cells)) was determined by subtracting the uptake clearance in the presence of excess unlabeled substrate (300 μM) ($CL_{(2\ min\text{-}0.5\ min),excess}$) from that in the presence of 1 □M substrate ($CL_{(2\ min\text{-}0.5\ min),tracer}$) as shown in (Eq. I-2).

$$CL_{(2\,\mathrm{min}-0.5\,\mathrm{min})} = \frac{V_{d,2\,\mathrm{min}} - V_{d,0.5\,\mathrm{min}}}{2-0.5} \qquad \text{(Eq. I-1)}$$

$$CL_{hep} = CL_{(2\mathrm{min}-0.5\mathrm{min}),tracer} - CL_{(2\mathrm{min}-0.5\mathrm{min}),excess} \qquad \text{(Eq. I-2)}$$

Kinetic parameters were obtained using the following equation:

$$v = \frac{V_{\max} \times S}{K_m + S} + P_{dif} \times S \qquad \text{(Eq. I-3)}$$

where v is the initial uptake velocity of substrate (pmol/min/mg protein(or 10^6 cells)), S is the substrate concentration in the incubation buffer (μM), K_m is the

Michaelis-Menten constant (μM), V_{max} is the maximum uptake velocity (pmol/min/mg protein(or 10^6 cells)) and P_{dif} is the nonspecific uptake clearance (μL/min/mg protein(or 10^6 cells)). The uptake data were fitted to this equation by a nonlinear least-squares method using a MULTI program (Yamaoka et al., 1981). The input data were weighted as the reciprocal of the observed values and the Damping Gauss Newton method was used as the fitting algorithm.

Results

Uptake of taurocholate, UDCA and its conjugates by human OATP1B1-, OATP1B3- and OAT2-expressing HEK293 cells

The time course of the uptake of UDCA and its conjugates, TUDC and GUDC, by human OATP1B1- and OATP1B3-expressing HEK293 cells are shown in Fig. I-2A, B and C, respectively. TUDC and GUDC showed significantly greater uptake in HEK293 cells expressing OATP1B1 or OATP1B3 compared with vector-transfected cells. The time-dependent uptake of UDCA was observed even in vector-transfected cells and transfection of OATP1B1 or OATP1B3 to HEK293 cells did not enhance the intracellular accumulation of UDCA. As previously described (Hagenbuch and Meier, 2003), significant uptake of taurocholate by our OATP1B1 and OATP1B3 expression system was also observed (Fig. I-2D). On the other hand, the significant uptake of UDCA, TUDC, GUDC and TCA was not observed in human OAT2-transfected cells compared with vector-transfected cells (Fig. I-6).

Because the uptake of TUDC and GUDC was linear up to 2 min (Fig. I-2B, C), the initial uptake was investigated as the uptake for 2 min at various substrate concentrations (Fig. I-3). The uptake of TUDC and GUDC by HEK293 cells

expressing OATP1B1 and OATP1B3 was saturated at higher concentration. The Eadie-Hofstee plots shown in Fig. I-3 indicate that the uptake of TUDCA and GUDCA by OATP1B1- and OATP1B3-expressed HEK293 cells consists of one saturable component. The K_m and V_{max} values are summarized in Table I-1A. The uptake clearance (V_{max}/K_m) of GUDC by OATP1B1- and OATP1B3-expressed cells was about 3 times higher than that of TUDC.

Uptake of taurocholate, UDCA and its conjugates by human NTCP-expressing HEK293 cells

The time course of the uptake of UDCA and its conjugates, TUDC and GUDC, by human NTCP-expressing HEK293 cells is shown in Fig. I-4A, B and C, respectively. TUDC and GUDC were taken up by HEK293 cells expressing human NTCP more rapidly than vector-transfected cells. NTCP-mediated significant uptake of UDCA was observed, although it was very low. Eadie-Hofstee plots of the NTCP-mediated uptake of TUDC and GUDC are shown in Fig. I-5. It appears that GUDC exhibits biphasic saturation kinetics, while TUDC has only one saturable component. The K_m and V_{max} values are listed in Table I-1B.

Uptake of taurocholate, UDCA and its conjugates by human cryopreserved hepatocytes

The uptake of UDCA, TUDC, GUDC and taurocholate by human cryopreserved hepatocytes prepared from three independent donors was investigated. Typical uptake time courses by human cryopreserved hepatocytes from one donor (Lot. OCF) are shown in Fig. I-7. Time-dependent uptake of all compounds was observed and this decreased in the presence of an excess of unlabeled compounds (Fig. I-7). The proportion of the saturable uptake clearance of UDCA, TUDC, GUDC and taurocholate calculated as explained in the **Materials & Methods** under tracer conditions was 64, 74, 47 and 43 % of the total uptake clearance, respectively. Replacement of Na^+ with choline in the incubation buffer resulted in a partial reduction of their uptake (Fig. I-7). The results of the uptake experiments using the other two lots of hepatocytes showed the same pattern as described above. The saturable uptake clearance of each compound in the three lots of human hepatocytes in the presence or absence of Na^+ is given in Table I-2. The average Na^+-dependent fraction of the total uptake clearance of UDCA, TUDC, GUDC

and taurocholate obtained from the three lots of hepatocytes was 49, 55, 21 and 63 %, respectively.

Concentration-dependence of Na^+-dependent and -independent uptake clearance of UDCA and its conjugates by human cryopreserved hepatocytes

Fig. I-8 shows the Eadie-Hofstee plots of the uptake of UDCA, TUDC and GUDC in the presence or absence of Na^+ using human cryopreserved hepatocytes of OCF, the lot with the highest uptake activity. One saturable and one non-saturable model can explain the concentration dependency of each experiment so well. Kinetic parameters for UDCA, TUDC and GUDC are summarized in Table I-3. The K_m and V_{max} values for the Na^+-independent uptake of all compounds were smaller than those for uptake in the presence of Na^+.

Discussion

In this study, we focused on the hepatic uptake of UDCA and its conjugates, which is one of the important processes in their enterohepatic circulation. To clarify the involvement of transporters and their contributions to the hepatic uptake, we performed kinetic analyses using transporter-expressing HEK293 cells and human cryopreserved hepatocytes.

First we checked the involvement of transporters in the hepatic uptake of UDCA and its conjugates in human NTCP, OATP1B1, OATP1B3 and OAT2-expressing HEK293 cells. It is generally believed that NTCP is responsible for the Na^+-dependent uptake, while OATP1B1 and OATP1B3 are mainly involved in the Na^+-independent uptake. Our results indicate that NTCP, OATP1B1 and OATP1B3 transport TUDC and GUDC in a saturable manner. The K_m values for OATP1B1 were lower than those for OATP1B3. The K_m values of TUDC and GUDC obtained in the present study were very similar to reported K_m values for rat Oatps(Eckhardt et al., 1999; Reichel et al., 1999; Walters et al., 2000). In the case of NTCP, the uptake of GUDC could be explained by a two-saturable model, while TUDC exhibited monophasic saturation. The K_m value of TUDC for human NTCP was lower than that for rat

Ntcp (14 μM)(Schroeder et al., 1998). Comparing the reported K_m values of taurocholate for NTCP (6.2, 7.9 μM)(Hagenbuch and Meier, 1994; Kim et al., 1999) and OATP1B1 (10, 33.8 μM)(Hsiang et al., 1999; Cui et al., 2001), TUDC and GUDC showed higher affinity than taurocholate in human NTCP and OATP1B1 and the relative uptake clearance of TUDC and GUDC was higher than that of taurocholate (Figs. I-2 and 4).

On the other hand, NTCP showed a very small but significant uptake of UDCA, while no significant uptake via OATP1B1 and OATP1B3 was observed. This result was consistent with the recent report showing that rat Oatp1a1 can transport TUDC and GUDC, but not UDCA(Hata et al., 2003). We observed time-dependent association of UDCA in the control cells. Because the uptake of 1 μM UDCA was not significantly changed even in the presence of 300 μM UDCA or 300 μM probenecid, which was used as a typical inhibitor of organic anion transport systems, and the uptake at 37 °C was not very different from that at 4 °C (data not shown), we confirmed that UDCA is taken up not by energy-driven active transport mechanism for organic anion in HEK293 cells.

Next, we characterized the uptake of UDCA and its conjugates by human cryopreserved hepatocytes. Although some inter-batch differences were

observed, more than half of the uptake clearance was saturable, which suggests the importance of transporters in the hepatic uptake of UDCA and its conjugates. The Na^+-dependent fraction in the overall uptake was 63 % for taurocholate, and about 50 % for TUDC and UDCA. On the other hand, it is interesting that Na^+-dependent fraction in overall hepatic uptake of GUDC was only about 20%, which was relatively low compared with UDCA and TUDC. GUDC is the most important molecule as far as the enterohepatic circulation of UDCA is concerned because 70-80 % of orally administered UDCA is conjugated with glycine(Invernizzi et al., 1999). In rats, UDCA is extensively conjugated with taurine and TUDC undergoes enterohepatic circulation(Crosignani et al., 1996). The uptake of TUDC in isolated rat hepatocytes in the absence of Na^+ has been reported to be about one-thirteenth of that in the presence of Na^+(Takikawa et al., 1995), indicating that the contribution of the Na^+-dependent pathway to the uptake of TUDC in rat hepatocytes is greater than that in human hepatocytes. Taking these findings into consideration, it is possible that Na^+-dependent uptake of TUDC is responsible for the efficient enterohepatic circulation of UDCA in rats, while the Na^+-independent pathway is also important for the enterohepatic circulation of UDCA (as its glycine conjugate) in humans.

Then, we performed self-inhibition experiments in the presence and absence of Na^+ using human cryopreserved hepatocytes (Table. I-3). The K_m values of TUDC and GUDC uptake in the presence of Na^+ were higher than that of taurocholate (2-8 μM)(Shitara et al., 2003b), while those in the absence of Na^+ were close to those of OATPs. We have already developed a method for determining the contribution of OATP1B1 and OATP1B3 to the hepatic uptake of a variety of compounds(Hirano et al., 2004). Applying this method to the estimation, the contribution of OATP1B1 was almost the same as that of OATP1B3 to the hepatic uptake of UDCA conjugates. On the other hand, the K_m values of UDCA conjugates in the presence of Na^+ were greater than those of NTCP. It has been shown that the K_m value of taurocholate uptake in cryopreserved human hepatocytes (2-8 μM)(Shitara et al., 2003b) was comparable with that in human NTCP-expression systems (6.2, 7.9 μM)(Hagenbuch and Meier, 1994; Kim et al., 1999), implying that the saturation kinetics of taurocholate uptake in human hepatocytes could be explained by the result obtained from NTCP-expression system. Therefore, this discrepancy between the K_m values of UDCA conjugates in human hepatocytes and the NTCP expression system suggests that unknown transporters may be

responsible for the Na^+-dependent uptake of UDCA conjugates. Microsomal epoxide hydrolase (mEH) might be one of the candidates for the low affinity Na^+-dependent transport system because the K_m value of taurocholate uptake via mEH has been reported to be 26.3 μM(von Dippe et al., 1996), which is greater than that via NTCP (6 μM), although the functional significance of mEH is controversial.

Regarding the hepatic uptake of UDCA, it has been reported that the contributions of the Na^+-dependent and -independent pathways to its hepatic uptake were almost identical in isolated hamster hepatocytes, which is consistent with our results(Bouscarel et al., 1995). On the other hand, we did not see any significant uptake of UDCA via OATP1B1 and OATP1B3, which we expected to work as high-affinity Na^+-independent transport systems. Britz et al. have reported that Bamet-UD2 (cisplatin conjugated with two molecules of UDCA) can be taken up by OATP1A2 (OATP-A), OATP1B1 (OATP-C), organic cation transporter (OCT) 1, OCT2 and NTCP(Briz et al., 2002). Therefore, other transporters may play a role in the Na^+-independent uptake of UDCA. Moreover, the rank order of the Na^+-dependent uptake of UDCA and its conjugates in human hepatocytes was different from that in the NTCP

expression system. Further characterization of the UDCA transport mechanisms will be needed.

In humans, most of UDCA is conjugated with glycine and serum concentration of conjugated UDCA in portal venous blood was larger than that of unconjugated UDCA in gallstone patients treated with UDCA(Ewerth et al., 1985). Therefore, the clearance of GUDC may be one of the determinant factors for the pharmacokinetics of UDCA. We showed that the hepatic uptake of GUDC is mediated mainly by Na^+-independent carriers, such as OATP1B1 and OATP1B3, so the function of OATP1B1 and OATP1B3 may partly determine the pharmacokinetics of UDCA. Some single nucleotide polymorphisms (SNPs) in OATP1B1 and OATP1B3 changed the transport activity compared with wild type and especially SNPs in OATP1B1 markedly affected the pharmacokinetics of substrates of OATP1B1 such as pravastatin in clinical situations[31]. Therefore, the SNPs in these transporters may also alter the clinical pharmacokinetics of UDCA.

In conclusion, we confirmed that UDCA and its conjugates can be taken up in both a Na^+-dependent and Na^+-independent manner and that their uptake is saturable, indicating the involvement of transporters in the hepatic uptake of

UDCA and its conjugates in human cryopreserved hepatocytes. In particular, GUDC, which is the major component of UDCA administered clinically, can be transported mainly in a Na^+-independent manner in human hepatocytes. From the results of the transport assay using expression systems, UDCA can be recognized by NTCP, but not OATP1B1 and OATP1B3, while conjugated UDCA can be transported by at least NTCP, OATP1B1 and OATP1B3. We suggest that these transporters may play an important role in the enterohepatic circulation of UDCA and its subsequent therapeutic effects.

Tables and Figures

(A)

	OATP1B1			OATP1B3		
	Km [μM]	Vmax [pmol/min/mg protein]	Vmax/Km [μL/min/mg protein]	Km [μM]	Vmax [pmol/min/mg protein]	Vmax/Km [μL/min/mg protein]
TUDC	7.47 ± 0.99	8.71 ± 1.02	1.17 ± 0.21	15.9 ± 3.3	40.2 ± 7.6	2.54 ± 0.71
GUDC	5.17 ± 0.71	20.6 ± 2.5	3.99 ± 0.73	24.7 ± 1.8	195 ± 13	7.90 ± 0.79

(B)

	NTCP		
	Km [μM]	Vmax [pmol/min/mg protein]	Vmax/Km [μL/min/mg protein]
TUDC	3.49 ± 0.34	10.1 ± 0.6	2.90 ± 0.31
GUDC	0.376 ± 0.174 25.3 ± 1.8	0.358 ± 0.145 36.7 ± 1.2	0.953 ± 0.587 1.45 ± 0.11

Table. I-1 Kinetic parameters of OATP1B1, OATP1B3 (A) and NTCP- (B) mediated uptake of TUDC and GUDC.

The uptake of TUDC and GUDC into OATP1B1, OATP1B3 (A) and NTCP- (B) expressing HEK293 cells was measured at different substrate concentrations. Kinetic parameters were obtained by fitting the Michaelis-Menten equation as described in **Materials & Methods**. Data represent the mean ± computer calculated S.D.

substrate		Lot. OCF	Lot. ETR	Lot. 094	average
TCA	Na+(+)	10.7±2.3	4.01±0.93	7.49±0.28	7.40±0.83
	Na+(−)	3.64±4.30	1.05±1.08	3.62±1.52	2.77±1.56
	Na+−dependent	7.07±4.90	2.97±1.43	3.87±1.55	4.64±1.78
UDCA	Na+(+)	42.4±8.2	21.5±4.7	9.17±3.06	24.4±3.3
	Na+(−)	15.7±9.8	16.1±2.3	5.57±2.74	12.5±3.5
	Na+−dependent	26.7±12.8	5.43±5.25	3.59±4.11	11.9±4.8
TUDC	Na+(+)	21.5±7.7	7.80±2.01	6.43±2.62	11.9±2.8
	Na+(−)	9.86±3.66	4.51±0.60	1.79±1.25	5.39±1.30
	Na+−dependent	11.7±8.5	3.29±2.09	4.65±2.91	6.55±3.07
GUDC	Na+(+)	11.2±3.3	3.79±2.57	3.24±1.65	6.08±1.50
	Na+(−)	8.70±2.46	1.69±0.95	3.94±3.83	4.78±1.55
	Na+−dependent	2.52±4.14	2.10±2.73	(<0)	1.30±2.16

(Unit: μL/min/10^6cells)

Table. I-2 Na^+-dependent and –independent uptake of TCA, UDCA, TUDC and GUDC in human cryopreserved hepatocytes.

The uptake of TCA, UDCA, TUDC and GUDC in three independent lots of human cryopreserved hepatocytes was measured in the presence and absence of Na^+. Na^+-dependent uptake clearance was calculated by subtracting the clearance in the absence of Na^+ from that in the presence of Na^+. Data represent the mean ± S.E. of three separate determinations.

(A)

	$Na^+(+)$			
	Km [μM]	Vmax [pmol/min/10^6 cells]	Vmax/Km [μL/min/10^6 cells]	Pdif [μL/min/10^6 cells]
UDCA	42.1 ± 13.1	1860 ± 670	44.3 ± 21.1	15.6 ± 3.1
TUDC	21.2 ± 13.0	453 ± 266	21.4 ± 18.9	25.3 ± 2.3
GUDC	84.1 ± 33.5	1350 ± 721	16.0 ± 10.7	9.31 ± 2.72

(B)

	$Na^+(-)$			
	Km [μM]	Vmax [pmol/min/10^6 cells]	Vmax/Km [μL/min/10^6 cells]	Pdif [μL/min/10^6 cells]
UDCA	4.30 ± 2.98	66.9 ± 38.3	15.5 ± 14.0	11.2 ± 1.2
TUDC	15.2 ± 27.3	122 ± 221	8.05 ± 20.54	13.5 ± 2.7
GUDC	32.8 ± 14.1	366 ± 164	11.1 ± 6.9	5.40 ± 1.05

Table. I-3 Kinetic parameters of the uptake of UDCA, TUDC and GUDC in human cryopreserved hepatocytes in the presence (A) or absence (B) of Na^+.

The uptake of UDCA, TUDC and GUDC into human cryopreserved hepatocytes (Lot. OCF) was measured in the presence (A) or absence (B) of Na^+. Kinetic parameters were obtained by fitting the one-saturable one-non-saturable model as described in **Materials & Methods**. Data represent the mean ± computer calculated S.D.

(A)

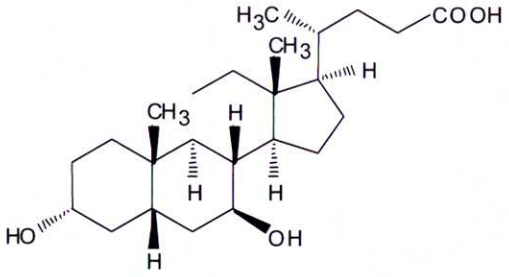

(B)

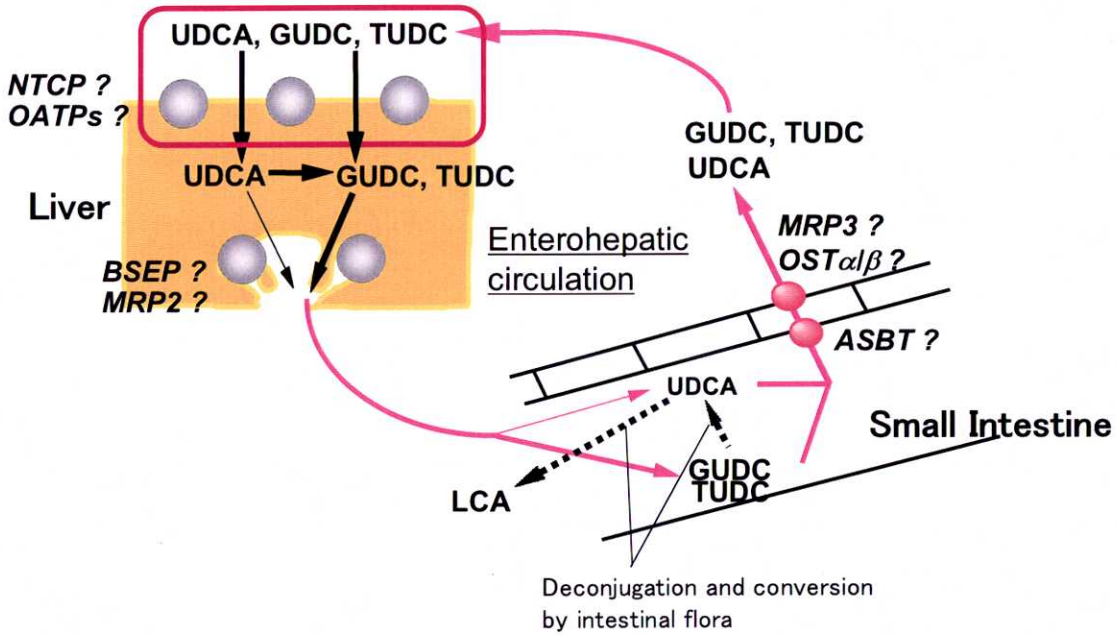

Fig. I-1 Chemical structure of UDCA (A) and schematic diagram of the hepatobiliary transport of UDCA and its conjugates (B)

(B)
LCA: lithocholate
ASBT: apical sodium-dependent bile salt transporter
OST: organic solute carrier

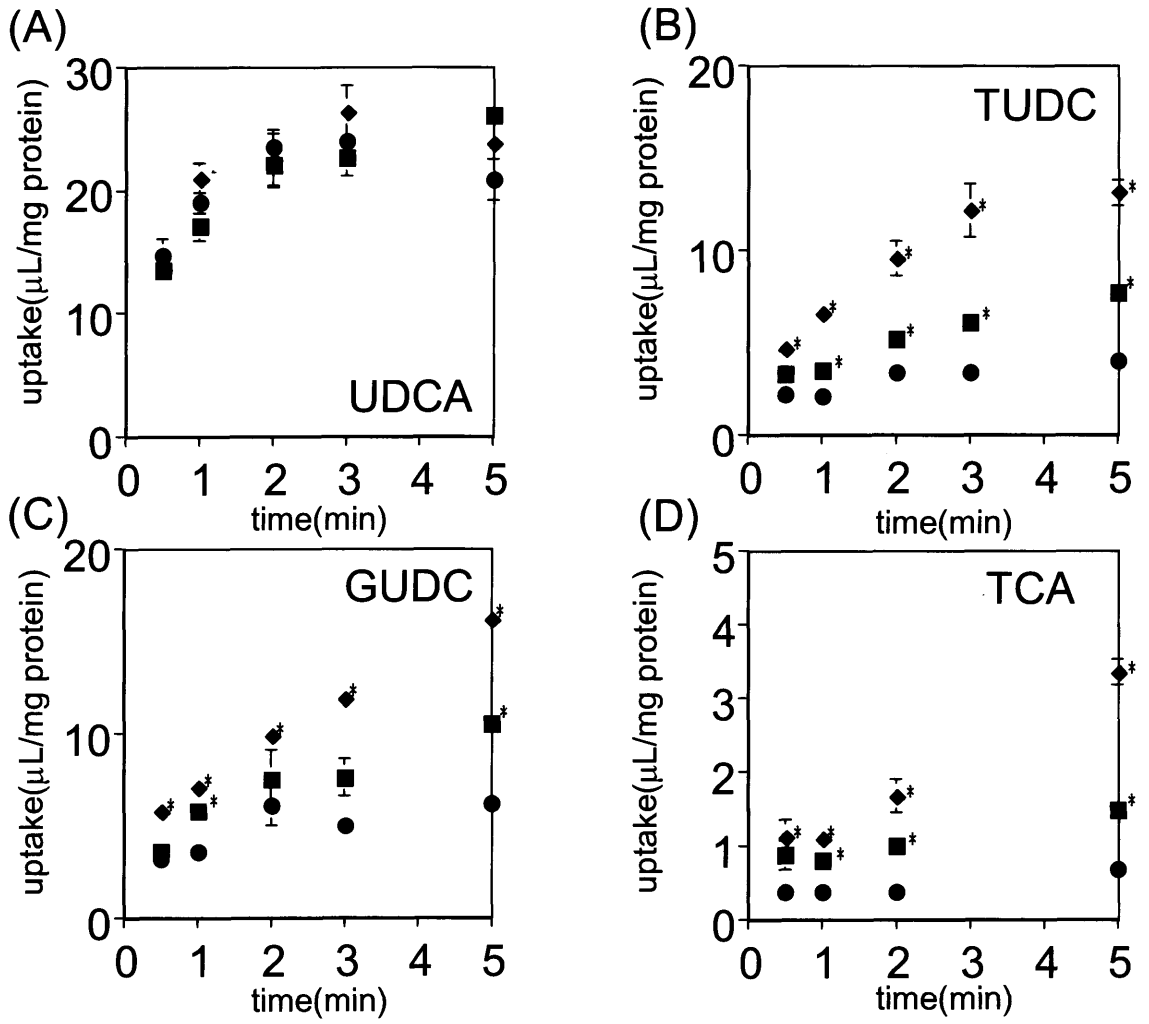

Fig. I-2 Time course of the uptake of UDCA (A) , TUDC (B), GUDC (C) and taurocholate (TCA) (D) by OATP1B1-expressing, OATP1B3-expressing and vector-transfected HEK293 cells

The concentration of bile acids is 1 μM. Uptake in OATP1B1-expressing cells is indicated by squares, in OATP1B3-expressing cells by diamonds, and in vector-transfected cells by circles. Each data point and bar represents the mean ± S.E. (n = 3). *p < 0.05, significantly different from vector-transfected cells by Student's t test.

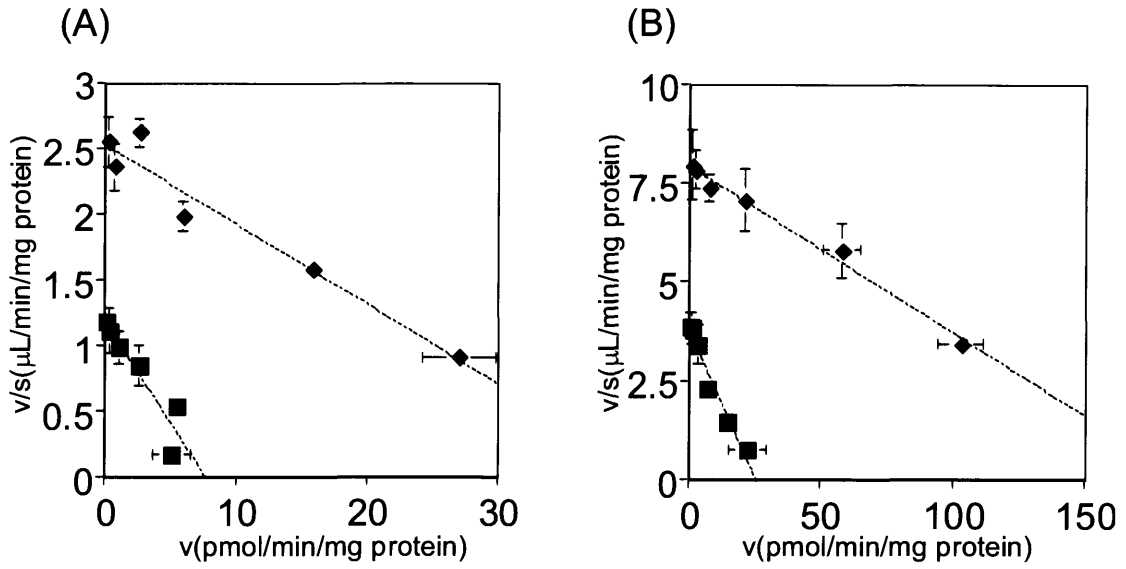

Fig. I-3 Eadie-Hofstee plots of the OATP1B1- (A) and OATP1B3- (B) mediated uptake of TUDC and GUDC

The concentration-dependence (1-100 μM) of OATP1B1- (squares) and OATP1B3-mediated uptake (diamonds) of TUDC (A) and GUDC (B) was determined. Transporter-mediated uptake was calculated by subtracting the uptake into vector-transfected cells from that into transporter-expressing cells. Each data point and bar represents the mean ± S.E. (n = 3).

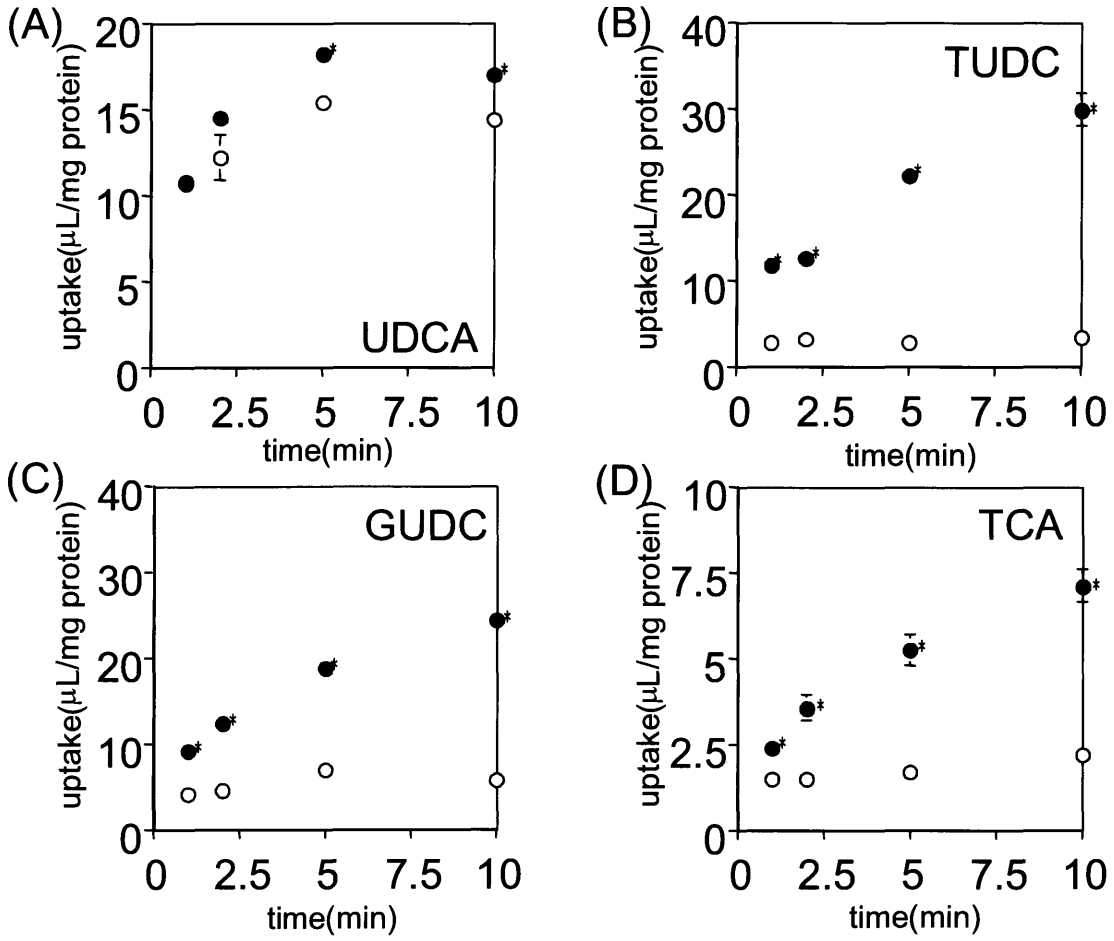

Fig. I-4 Time course of the uptake of UDCA (A), TUDC (B), GUDC (C) and taurocholate (TCA) (D) by NTCP-expressing and vector-transfected HEK293 cells

The concentration of bile acids is 1 μM. Uptake in NTCP-expressing cells is indicated by closed circles and in vector-transfected cells by open circles. Each data point and bar represents mean ± S.E. (n = 3). *$p < 0.05$, significantly different from vector-transfected cells by Student's *t* test.

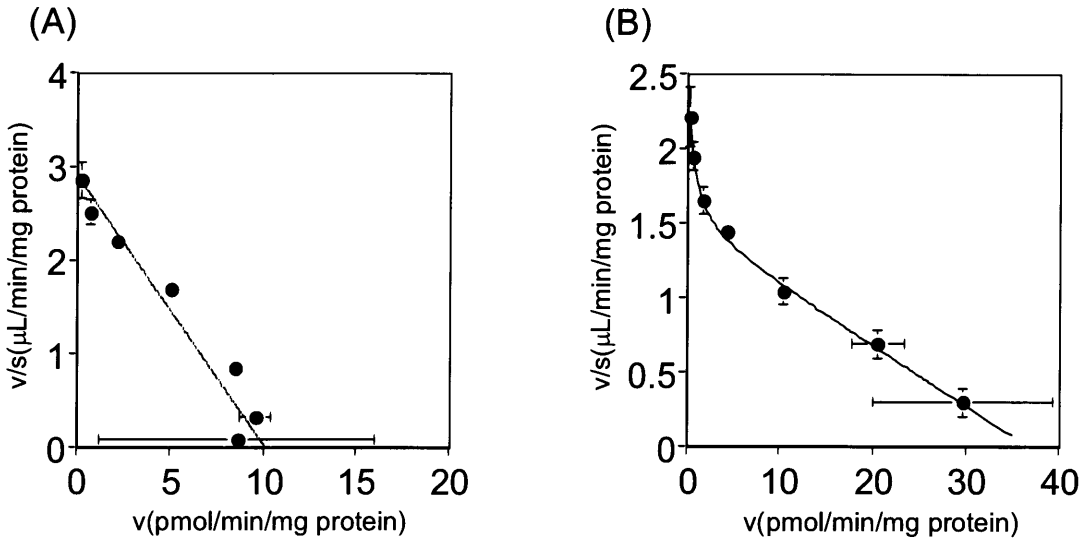

Fig. I-5 Eadie-Hofstee plots of the NTCP-mediated uptake of TUDC (A) and GUDC (B)

The concentration-dependence (1-100 μM) of NTCP-mediated uptake of TUDC (A) and GUDC (B) was determined. NTCP-mediated uptake was calculated by subtracting the uptake into vector-transfected cells from that into NTCP-expressing cells. Each data point and bar represents mean ± S.E. (n = 3).

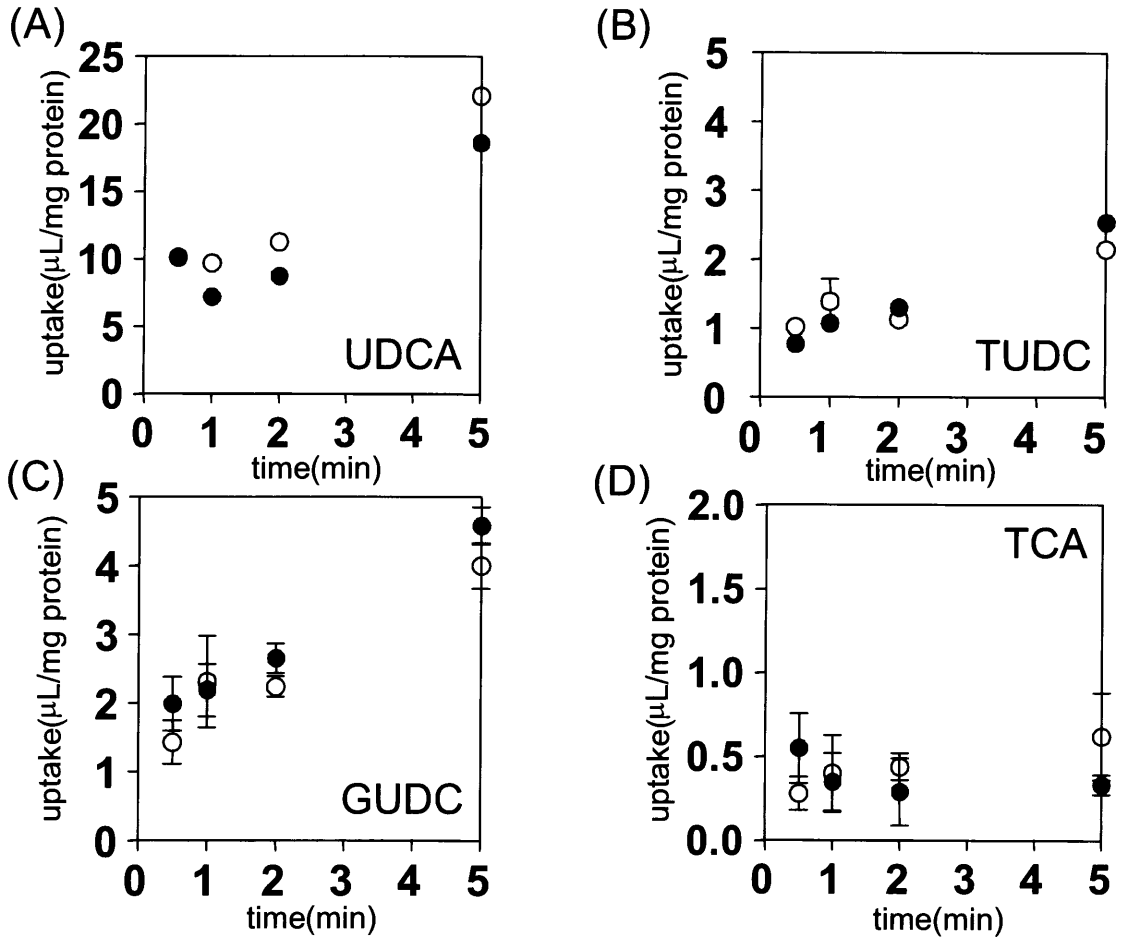

Fig. I-6 Time course of the uptake of UDCA (A), TUDC (B), GUDC (C) and taurocholate (TCA) (D) by human OAT2-expressing and vector-transfected HEK293 cells

The concentration of bile acids is 1 μM. Uptake in human OAT2-expressing cells is indicated by closed circles and in vector-transfected cells by open circles. Each data point and bar represents mean ± S.E. (n = 3).

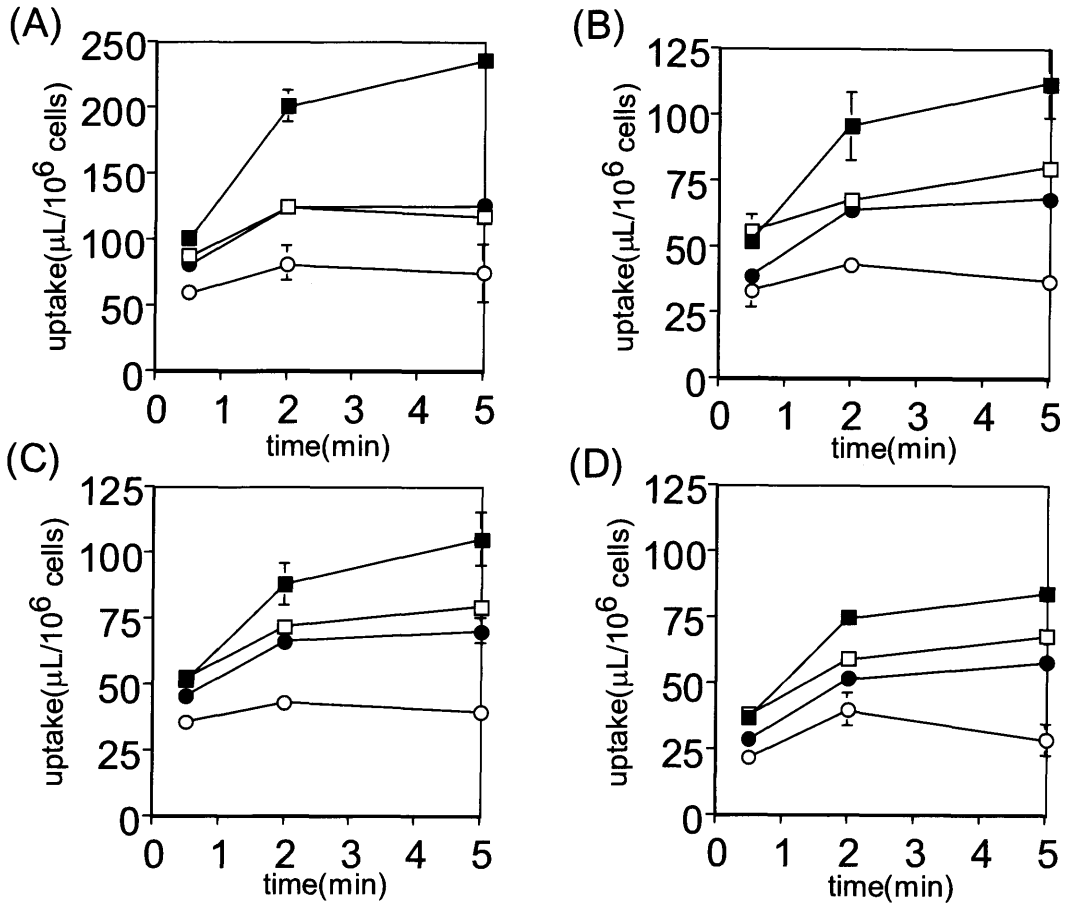

Fig. I-7 Time-profiles for the uptake of UDCA (A), TUDC (B), GUDC (C) and TCA (D) in human cryopreserved hepatocytes (Lot. OCF)

Uptake of UDCA (A), TUDC (B), GUDC (C) and taurocholate (TCA) (D) into human cryopreserved hepatocytes was measured by incubating cells with 1 μM (closed symbols) or 300 μM (open symbols) of each ligand at 37°C in the presence (squares) or absence of Na^+ (circles). The viability of the human hepatocytes used in this experiment was 70 %. Each time point and bar represents mean ± S.E. of 3 separate determinations.

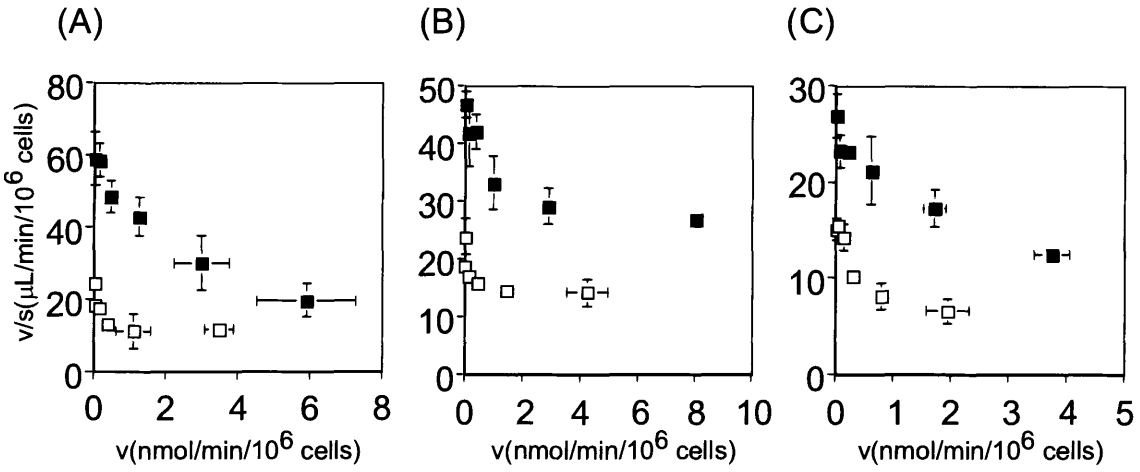

Fig. I-8 Concentration-dependence of the uptake of UDCA (A), TUDC (B) and GUDC (C) in human cryopreserved hepatocytes (Lot. OCF) in the presence or absence of Na^+

The uptake of UDCA (A), TUDC (B) and GUDC (C) into human cryopreserved hepatocytes was measured in the presence (closed square) or absence of Na^+ (open square). The clearance at each concentration (1-300 μM) was determined by (Eq. I-1) shown in the **Materials & Methods**. The viability of the human hepatocytes used in this experiment was 70 %.
Each time point and bar represents mean ± S.E. of 3 separate determinations.

Part II

Effects of OATP1B1 haplotype on pharmacokinetics of pravastatin, valsartan and temocapril

Abstract

Recent reports have shown that genetic polymorphisms in OATP1B1 have an effect on the pharmacokinetics of drugs. However, the impact of OATP1B1*1b alleles, whose frequency is high in all ethnicities, on the pharmacokinetics of substrate drugs is not known after complete separation of subjects with OATP1B1*1a and *1b. Furthermore, the correlation between clearances of OATP1B1 substrate drugs in individuals has not been characterized. So, to investigate the effect of genetic polymorphism of OATP1B1, particularly the *1b allele, on the pharmacokinetics of three anionic drugs, pravastatin, valsartan and temocapril in Japanese subjects, 23 Japanese healthy volunteers were enrolled in a three-period crossover study. In each period, after a single oral administration of pravastatin, valsartan or temocapril, plasma and urine were collected for up to 24 hours. As a result, the plasma AUC of pravastatin in *1b/*1b carriers (47.4 ± 19.9 ng*hr/mL) was 65% of that in *1a/*1a carriers (73.2 ± 23.5 ng*hr/mL; $p = 0.049$). *1b/*15 carriers (38.2 ± 15.9 ng*hr/mL) exhibited a 45 % lower plasma AUC than *1a/*15 carriers (69.2 ± 23.4 ng*hr/mL; $p = 0.024$). In the case of valsartan, we observed the similar trend as with pravastatin, although the difference was not statistically significant (*1b/*1b (9.01 ± 3.33

μg*hr/mL) vs *1a/*1a (12.3 ± 4.6 μg*hr/mL); p =0.171, *1b/*15 (6.31 ± 3.64 μg*hr/mL) vs *1a/*15 (9.40 ± 4.34 μg*hr/mL); p =0.213). The plasma AUC of temocapril also showed a similar trend (*1b/*1b (12.4 ± 4.1 ng*hr/mL) vs *1a/*1a (18.5 ± 7.7 ng*hr/mL); p =0.061, *1b/*15 (16.4 ± 5.0 ng*hr/mL) vs *1a/*15 (19.0 ± 4.1 ng*hr/mL); p =0.425), while that of temocaprilat (active form of temocapril) was not significantly affected by the haplotype of OATP1B1. Interestingly, the plasma AUC of valsartan and temocapril in each subject was significantly correlated with that of pravastatin (R = 0.630 and 0.602; $p < 0.01$). The renal clearance remained unchanged for each haplotype for all drugs. Therefore, these results indicated that the major clearance mechanism of pravastatin, valsartan and temocapril appears to be similar and OATP1B1*1b is one of the determinant factors governing the interindividual variability in the pharmacokinetics of pravastatin and, possibly, valsartan and temocapril.

Introduction

The administration of the same dose of a drug sometimes results in large inter-individual differences in the pharmacokinetics and subsequent pharmacological and toxicological effects. The pharmacokinetics of certain drugs is dominated by absorption, disposition, metabolism and elimination and many molecules, such as metabolic enzymes and transporters, have been reported to be involved in each process. Recently, polymorphisms in each molecule have been identified and many *in vitro* and clinical studies have demonstrated that some of them are associated with a change in the expression and function of molecules and the pharmacokinetics of drugs. Although there is much information regarding metabolic enzymes like cytochrome P450 and phase II conjugation enzymes, the clinical significance of the genetic polymorphisms in transporters is not well understood.

Organic anion transporting polypeptide 1B1 (OATP1B1; formerly called OATP-C/OATP2) is exclusively expressed in the liver and located on the basolateral membrane(Abe et al., 1999; Hsiang et al., 1999; Konig et al., 2000). Some reports have indicated that OATP1B1 can transport a wide variety of compounds including clinically-important drugs such as

3-hydroxy-3-methylglutaryl-coenzyme A (HMG-CoA) reductase inhibitors(Hsiang et al., 1999; Shitara et al., 2003a; Hirano et al., 2004), which suggests that OATP1B1 may be responsible for the hepatic uptake of various kinds of anionic drugs, which efficiently accumulate in liver. Hepatic clearance consists of intrinsic clearances of hepatic uptake, sinusoidal efflux, metabolism and biliary excretion. From the viewpoint of pharmacokinetics, a change in the uptake process will directly affect the overall hepatic clearance, regardless of the absolute values of each intrinsic clearance(Shitara et al., 2005). Therefore, genetic polymorphisms in OATP1B1 may have an effect on the hepatic clearance of OATP1B1 substrates.

Several genetic polymorphisms in OATP1B1 have been reported and *in vitro* studies have shown that some of them reduce the transport capability of several substrates in OATP1B1 variant-expressing cells(Tirona et al., 2001; Iwai et al., 2004; Kameyama et al., 2005). Among these, previous studies have focused on two mutations, Asn130Asp and Val174Ala, because they are frequently observed in all ethnic groups investigated previously and their allele frequencies show some ethnic differences(Tirona et al., 2001; Nishizato et al., 2003), which may cause an ethnic difference in the pharmacokinetics of OATP1B1 substrates.

Interestingly, Nishizato et al. demonstrated that Val174Ala was tightly linked with Asn130Asp and formed a haplotype referred to as OATP1B1*15 in Japanese. In addition, after oral administration of pravastatin, healthy Japanese volunteers with the *15 allele showed an increase in the plasma AUC of pravastatin(Nishizato et al., 2003). This result was supported by *in vitro* analysis showing that the intrinsic V_{max} value normalized by the expression level for OATP1B1*15 variant was drastically reduced compared with OATP1B1*1a(Tirona et al., 2001; Iwai et al., 2004; Kameyama et al., 2005). Subsequently, two clinical studies showed that the Val174Ala mutation also increased the plasma AUC of pravastatin in Caucasians(Mwinyi et al., 2004; Niemi et al., 2004). Very recently, Niemi et al. reported that the pharmacokinetics of fexofenadine and repaglinide were also affected by the Val174Ala mutation(Niemi et al., 2005b). These results suggest that the Val174Ala mutation in OATP1B1 reduces the transport function. On the other hand, Mwinyi et al. showed that the plasma AUC of pravastatin in subjects with *1a/*1b (Asn130Asp) or *1b/*1b alleles tended to be lower than that in *1a homozygotes(Mwinyi et al., 2004). However, they didn't completely separate the subjects with *1b allele from those with *1a allele, and so we cannot directly

compare the effect of *1b allele with that of *1a. The allele frequency of OATP1B1*1b was reported to be high and showed some ethnic differences (e.g. European American (n=49): 0.30(Tirona et al., 2001), African American (n=44): 0.74(Tirona et al., 2001), Japanese (n=120): 0.63(Nishizato et al., 2003)), implying that this might cause the ethnic differences of the pharmacokinetics of drugs. Therefore, we were particularly interested in the effect of the Asn130Asp variant of OATP1B1 on the pharmacokinetics of three drugs, pravastatin, valsartan and temocaprilat, and we classified the subjects into 4 groups; *1a/*1a, *1b/*1b, *1a/*15, *1b/*15 to directly investigate the difference in the pharmacokinetics of the subjects with *1a and *1b (*1a/*1a vs *1b/*1b and *1a/*15 vs *1b/*15).

Valsartan is a novel angiotensin II receptor antagonist and temocapril is an angiotensin converting enzyme (ACE) inhibitor (Fig. II-2B,C). Drugs in these categories are widely used for the treatment of hypertension. Valsartan is mainly eliminated via the liver. Valsartan itself is pharmacologically active and is thought to be excreted into the bile in unchanged form without extensive metabolism(Israili, 2000). Because of its hydrophilicity and carboxyl moiety, some organic anion transporters may be involved in the hepatic clearance of

valsartan. Temocapril is an esterified prodrug and rapidly converted to the active metabolite, temocaprilat, by carboxyl esterase(Oizumi et al., 1988)(Fig. II-2C). Temocaprilat is mainly excreted into bile, while active metabolites of other ACE inhibitors such as enalaprilat are mainly excreted into urine because temocaprilat, but not enalaprilat, can interact with multidrug resistance associated protein 2 (Mrp2), which is an efflux transporter located on the apical membrane(Ishizuka et al., 1997). Sasaki et al. demonstrated that transcellular vectorial transport of temocaprilat was observed in OATP1B1/MRP2 double transfected cells, suggesting that temocaprilat is a substrate of OATP1B1(Sasaki et al., 2002).

Therefore, the purpose of this study was to clarify the importance of the OATP1B1 haplotype, especially *1b allele, in the pharmacokinetics of OATP1B1 substrates, pravastatin, valsartan and temocaprilat, and to check whether the clearances of OATP1B1 substrate drugs in each subject are well correlated with one another in healthy Japanese volunteers.

Materials & Methods

Subjects. 23 healthy Japanese male volunteers participated in this clinical study (Fig. II-1). They were recruited from a population of 100 Japanese male volunteers, whose OATP1B1 haplotype was pre-screened after obtaining written informed consent. The genotyping method of OATP1B1 has been described previously(Nishizato et al., 2003). The haplotypes of OATP1B1 in the 23 participants were *1a/*1a (n = 5), *1a/*15 (n = 6), *1b/*1b (n = 7) and *1b/*15 (n = 5). The age of the participants was between 20 and 35. Each participant had a body weight of between 50 and 80 kg, and a body mass index of between 17.6 and 26.4 kg/m^2. Within 1 month before starting this clinical study, a medical history was obtained from the participants who then underwent a physical examination, electrocardiography, routine blood testing and urinalysis. They were also screened for narcotic drugs and psychotropic substances. This allowed us to confirm that all the subjects were able to participate in this study.

Study design. This study protocol was approved by the Ethics Review Board both in the Graduate School of Pharmaceutical Sciences, the University of Tokyo and in Kannondai Clinic. All participants provided their written informed consent.

All subjects took part in the three-period crossover trial and received pravastatin, valsartan and temocapril in a random sequence (Fig. II-1). There was a washout period of one week between each administration. In each period, subjects came to the clinic the day before the drug administration. After an overnight fast, each subject received 10 mg pravastatin sodium (Mevalotin tablet; Sankyo Co., Ltd., Tokyo, Japan), 2 mg temocapril hydrochloride (Acecol tablet; Sankyo Co., Ltd.), or 40 mg valsartan (Diovan tablet; Novartis AG, Basel, Switzerland). Venous blood samples (each 7 mL) were collected in tubes containing heparin before and at 0.25, 0.5, 0.75, 1, 2, 4, 6, 8, 12 and 24 hours after drug administration. Urine samples were collected for 24 hours. Plasma was separated by centrifugation. Plasma and urine samples were stored at -80 °C until analysis. Alcohol, grapefruit juice, St. John's Wort and other drugs were not permitted from two days before admission to the clinic to the end of the study period and smoking was prohibited during the study period. During the study periods, standardized meals were served to all subjects at scheduled times. For the safety of subjects, after the end of each period, all subjects were given a physical examination and routine blood testing and urinalysis were carried out.

Quantification of pravastatin and its metabolite, RMS-416, in plasma and urine. Pravastatin and RMS-416 in plasma and urine were measured by liquid chromatography-tandem mass spectrometry as described in an earlier report(Kawabata et al., 2005). One mL of plasma was mixed with 100 μL internal standard (R-122798, 800 ng/mL, prepared from Sankyo Co., Ltd.), 1 mL 10 % methanol and 300 μL 0.5 M phosphate buffer (pH 4.0). In addition, 0.5 mL urine was mixed with 50 μL internal standard (R-122798), 0.5 mL 10 % methanol and 300 μL 0.5 M phosphate buffer (pH 4.0). The mixture was applied to a Bond Elut C8 cartridge (200mg/3mL) (Varian, Inc., Harbor City, CA), washed twice with 3 mL 5 % methanol (plasma) or distilled water (urine) and eluted with 2 mL acetonitrile. The eluate was evaporated under nitrogen gas at 40 °C, mixed with 120 μL acetonitrile and ultrasonicated for 3 minutes. Then, 180 μL 10 mM ammonium acetate was added and aliquots (20 μL for plasma, 10 μL for urine) were injected into the liquid chromatography-tandem mass spectrometry system. Separation by HPLC was conducted using an Agilent 1100 series system (Agilent Technologies Inc., Palo Alto, CA) with an Inertsil ODS-3 column (4.6 x 150 mm; 5 μm) (GL Sciences Inc., Tokyo, Japan). The composition of the mobile phase was

acetonitrile/water/ammoniumacetate/formic acid/triethylamine (400/600/0.77/0.2/0.6; vol/vol/wt/vol/vol). The flow rate was 1 mL/min. Mass spectra were determined with an API-4000 tandem mass spectrometer (Applied Biosystems, MDS SCI EX, Foster City, CA) in the negative ion-detecting mode at the atmospheric pressure-chemical ionization interface. The turbo gas temperature was 600 °C. The samples were ionized by reacting with solvent-reactant ions produced by the corona discharge (-5.0 μA) in the chemical ionization mode. The precursor ions of pravastatin at a mass-to-charge ratio (m/z) 423.2, RMS-416 at m/z 423.2, and R-122798 at m/z 409.2 were admitted to the first quadrupole (Q1). After the collision-induced fragmentation in the second quadrupole (Q2), the product ions of pravastatin at m/z 321.1, RMS-416 at m/z 321.3, and R-122798 at m/z 321.4 were monitored in the third quadrupole (Q3). The peak area ratio of each compound to the corresponding internal standard was calculated with Analyst ver. 1.3.1 software (Applied Biosystems). The calibration curves were linear over the standard concentration range of 0.1 ng/mL to 100 ng/mL for pravastatin and RMS-416 in plasma, 20 ng/mL to 2000 ng/mL for pravastatin in urine, and 5 ng/mL to 500 ng/mL for RMS-416 in urine.

Quantification of valsartan in plasma and urine. One hundred μL plasma or urine was mixed with 100 μL internal standard ([$^2H_9$]-valsartan in 50 % methanol, 500 ng/mL, prepared from Novartis Pharma K.K.) and 300 μL 2 % trifluoroacetic acid (TFA) aqueous solution. The mixture was applied to a 96-well Empore Disk Plate C_{18} SD (Sumitomo 3M Limited, Tokyo, Japan), washed three times with 200 μL 1 % TFA aqueous solution, 1 % TFA in 5 % methanol and 1% TFA in 20 % methanol and eluted twice with 100 μL methanol. The eluate was evaporated under nitrogen gas at 40 °C and mixed with 100 μL (plasma) or 400 μL (urine) methanol/acetonitrile/0.1% TFA (35/20/45; vol/vol/vol) and ultrasonicated for 3 minutes. Then, 5 μL aliquots were injected into the liquid chromatography-tandem mass spectrometry system. Separation by HPLC was conducted using an Agilent 1100 series system (Agilent Technologies Inc.) with a Symmetry C_{18} column (2.1 x 30 mm; 3.5 μm) (Waters Corporation, Milford, MA). The composition of the mobile phase was methanol/acetonitrile/0.1% TFA (35/20/45; vol/vol/vol). The flow rate was 0.2 mL/min. Mass spectra were determined with an API-4000 tandem mass spectrometer (Applied Biosystems) in the positive ion-detecting mode at the electrospray ionization interface. The

turbo gas temperature was 500 °C and the spray voltage was 5500 V. The precursor ions of valsartan at m/z 436.1 and [$^2H_9$]-valsartan at m/z 445.1 were admitted to the first quadrupole (Q1). After the collision-induced fragmentation in the second quadrupole (Q2), the product ions of valsartan at m/z 291.1 and [$^2H_9$]-valsartan at m/z 300.1 were monitored in the third quadrupole (Q3). The peak area ratio of each compound to the corresponding internal standard was calculated with Analyst ver. 1.3.1 software (Applied Biosystems). The calibration curves were linear over the standard concentration range of 2 ng/mL to 5000 ng/mL for plasma and 20 ng/mL to 5000 ng/mL for urine.

Quantification of temocapril and temocaprilat in plasma and urine. Two hundred μL plasma was mixed with 200 μL internal standard ([$^2H_5$]-temocaprilat, 10 ng/mL, prepared from Sankyo Co., Ltd.), 2 mL 0.1 % formic acid and 200 μL methanol. Then, 500 μL urine was mixed with 200 μL internal standard ([$^2H_5$]-temocaprilat), 500 μL 0.5 % formic acid and 500 μL methanol. The mixture was applied to a Sep-Pak Vac PS-2 cartridge (200mg/3mL) (Waters Corporation), washed with twice with 3 mL distilled water and eluted twice with 3 mL methanol. The eluate was evaporated under nitrogen gas at 45 °C, mixed

with 280 μL methanol and ultrasonicated for 3 minutes. Then, 120 μL 0.2 % acetic acid was added and 10 μL aliquots were injected into the liquid chromatography-tandem mass spectrometry system. Separation by HPLC was conducted using an Agilent 1100 series system (Agilent Technologies Inc.) with a Symmetry C_{18} column (2.1 x 150 mm; 5 μm) (Waters Corporation). The composition of the mobile phase was methanol/water/acetic acid (700/300/2; vol/vol/vol). The flow rate was 0.2 mL/min. Mass spectra were determined with an API-4000 tandem mass spectrometer (Applied Biosystems) in the positive ion-detecting mode at the electrospray ionization interface. The turbo gas temperature was 600 °C and the spray voltage was 5500 V. The precursor ions of temocapril at m/z 477.0, temocaprilat at m/z 448.9, and [$^2H_5$]-temocaprilat at m/z 454.0 were admitted to the first quadrupole (Q1). After the collision-induced fragmentation in the second quadrupole (Q2), the product ions of temocapril at m/z 270.0, temocaprilat at m/z 269.8, and [$^2H_5$]-temocaprilat at m/z 269.9 were monitored in the third quadrupole (Q3). The peak area ratio of each compound to the corresponding internal standard was calculated with Analyst ver. 1.3.1 software (Applied Biosystems). The calibration curves were linear over the standard concentration range of 0.5 ng/mL to 200 ng/mL for

temocapril and temocaprilat in plasma, 1 ng/mL to 80 ng/mL for temocapril in urine, and 5 ng/mL to 400 ng/mL for temocaprilat in urine.

Uptake study using OATP1B1-expression system. The OATP1B1-expressing HEK293 cells and vector-transfected control cells have been established and transport study was carried out as described previously(Hirano et al., 2004). [^{3}H]-valsartan and unlabeled valsartan were kindly donated by Novartis Pharma K.K. (Basel, Switzerland) and [^{14}C]-temocaprilat and unlabeled temocaprilat were donated by Sankyo Co., Ltd. (Tokyo, Japan). Uptake was initiated by adding Krebs-Henseleit buffer containing tritium-labeled and unlabeled substrates after cells had been washed twice and preincubated with Krebs-Henseleit buffer at 37°C for 15 min. The Krebs-Henseleit buffer consisted of 118 mM NaCl, 23.8 mM $NaHCO_3$, 4.8 mM KCl, 1.0 mM KH_2PO_4, 1.2 mM $MgSO_4$, 12.5 mM HEPES, 5.0 mM glucose, and 1.5 mM $CaCl_2$ adjusted to pH 7.4. The uptake was terminated at a designated time by adding ice-cold Krebs-Henseleit buffer after removal of the incubation buffer. Then, cells were washed twice with 1 ml of ice-cold Krebs-Henseleit buffer, solubilized in 500 μl of 0.2 N NaOH, and kept overnight at 4°C. Aliquots

(500 μl) were transferred to scintillation vials after adding 250 μl of 0.4 N HCl. The radioactivity associated with the cells and incubation buffer was measured in a liquid scintillation counter (LS6000SE; Beckman Coulter, Fullerton, CA) after adding 2 ml of scintillation fluid (Clear-sol I; Nacalai Tesque, Kyoto, Japan) to the scintillation vials. The remaining 50 μl of cell lysate was used to determine the protein concentration by the method of Lowry with bovine serum albumin as a standard.

Transcellular transport study using double transfected cells. The transcellular transport study was performed as reported previously (Sasaki et al., 2002). Briefly, MDCKII cells were grown on Transwell membrane inserts (6.5 mm diameter, 0.4 μm pore size; Corning Coster, Bodenheim, Germany) at confluence for 3 days and the expression level of transporters was induced with 5 mM sodium butyrate for 2 days before the transport study. Cells were firstly washed with Krebs-Henseleit buffer (118 mM NaCl, 23.8 mM $NaHCO_3$, 4.83 mM KCl, 0.96 mM KH_2PO_4, 1.20 mM $MgSO_4$, 12.5 mM HEPES, 5.0 mM glucose, and 1.53 mM $CaCl_2$ adjusted to pH 7.4) at 37 °C. Subsequently, substrates were added in Krebs-Henseleit buffer either to the apical compartments (250 μl) or to

the basolateral compartments (1 ml). After a designated period, the aliquot of the incubation buffer in the opposite compartments (100 μl from apical compartment or 250 μl from basal compartment) was collected. The amount of estradiol-17β-glucuronide in the samples was determined by a liquid scintillation counter (LS 6000SE, Beckman Instruments, Inc., Fullerton, CA) and the amount of temocapril and RMS-416 in the samples was determined by LC/MS as mentioned below.

Quantification of temocapril in the Krebs-Henseleit buffer. 50 μL sample was mixed vigorously with 250 μL of ethyl acetate. 200 μL of supernatant was collected, dried up by centrifugal concentrator (TOMY, Tokyo, Japan) and dissolved in 40 μL dimethylsulfoxide. 30 μL aliquots were injected into the liquid chromatography-tandem mass spectrometry system. Separation by HPLC was conducted using a Waters Alliance 2695 Separations Module (Waters Corporation, Milford, MA) with an L-column ODS (2.1 x 150 mm; 5 μm) (Chemicals Evaluation and Research Institute, Tokyo, Japan). The composition of the mobile phase was acetonitrile/0.05% formic acid (40/60; vol/vol). The flow rate was 0.3 mL/min. Mass spectra were determined with a Micromass

ZQ2000 mass spectrometer (Waters Corporation) in the positive ion-detecting mode at the electrospray ionization interface. The source temperature and desolvation temperature were 100 °C and 350 °C, respectively. The capillary, cone and extractor voltage were 3200 V, 30 V and 5 V, respectively. The cone gas flow and desolvation gas flow were 65 L/h and 375 L/h. The mass spectrometer was operated in the selected ion monitoring mode (SIM) using positive ion, m/z 477.30 for temocapril. The retention time of temocapril was approximately 3.7 min. Standard curves were linear over the range of 3-300 nM.

Quantification of RMS-416 in the Krebs-Henseleit buffer. 60 μL sample was mixed vigorously with 60 μL of methanol including internal standard (0.5 μg/mL R-122798; kindly donated from Sankyo Co., Ltd.) and deproteinized by centrifugation for 10 min at 15,000 rpm at 4 °C. Then, 50 μL of supernatant was injected into the liquid chromatography-tandem mass spectrometry system. Separation by HPLC was conducted using a Waters Alliance 2695 Separations Module (Waters Corporation) with a Inertsil ODS-3 (4.6 x 150 mm; 5 μm) (GL Sciences Inc., Tokyo, Japan). The composition of the mobile phase was

acetonitrile/10 mM ammonium acetate (pH=4) (40/60; vol/vol). The flow rate was 0.3 mL/min. Mass spectra were determined with a Micromass ZQ2000 mass spectrometer (Waters Corporation) in the negative ion-detecting mode at the electrospray ionization interface. The source temperature and desolvation temperature were 100 °C and 350 °C, respectively. The capillary, cone and extractor voltage were 3200 V, 20 V and 5 V, respectively. The cone gas flow and desolvation gas flow were 65 L/h and 375 L/h. The mass spectrometer was operated in the selected ion monitoring mode (SIM) using respective positive ions, m/z 423.30 for RMS-416 and m/z 409.30 for R-122798 (internal standard). The retention time of RMS-416 and R-122798 was approximately 3.6 min and 2.6 min, respectively. Standard curves were linear over the range of 5-1000 nM.

Pharmacokinetic and statistical analyses. The area under the plasma concentration-time curve from time 0 to 24 hours (AUC_{0-24}) was calculated by the linear trapezoidal rule. Renal clearance (CL_r) was calculated by dividing the cumulative amount of drug in urine collected for 24 hours by the AUC_{0-24}. All pharmacokinetic data are given as the mean ± S.D. The statistical differences

between the data for each haplotype group were determined by analysis of variance (ANOVA) followed by Fisher's least significant difference test. $P < 0.05$ was considered to be statistical significant.

Results

Effect of OATP1B1 haplotype on the pharmacokinetics of pravastatin and its metabolite, RMS-416

After oral administration of pravastatin, the plasma concentration of pravastatin in subjects with OATP1B1*1b/*1b was lower than that in subjects with OATP1B1*1a/*1a (Fig. II-3A). Similarly, the plasma concentration in *1b/*15 subjects was lower than that in *1a/*15 subjects (Fig. II-3B). The mean AUC_{0-24} of pravastatin in *1b/*1b subjects was significantly lower than that in *1a/*1a subjects (65 % of *1a/*1a) and the AUC_{0-24} in *1b/*15 subjects was significantly lower than that in *1a/*15 subjects (55 % of *1a/*15) (Fig. II-3C, Table. II-1). In addition, the renal clearance (CL_r) was not significantly different among the haplotype groups (Table. II-1). Pravastatin was converted to RMS-416 by chemical epimerization (Fig. II-2A). Then, we also calculated the concentration of the sum of pravastatin and RMS-416 in plasma and urine. The AUC_{0-24} value of the sum of pravastatin and RMS-416 in *1b carriers tended to be lower than that in *1a carriers, while this value in *15 carriers tended to be higher than that in non-*15 carriers (Fig. II-4, Table. II-1). The renal clearance calculated from the sum of pravastatin and RMS-416 was not markedly different between each

haplotype group(Table. II-1).

Effect of OATP1B1 haplotype on the pharmacokinetics of valsartan

After oral administration of valsartan, the plasma concentration of valsartan in subjects with OATP1B1*1b/*1b was lower than that in subjects with OATP1B1*1a/*1a (Fig. II-5A) and the plasma concentration in *1b/*15 subjects was lower than that in *1a/*15 subjects (Fig. II-5B). Although the difference did not reach statistical significance, the average AUC_{0-24} of valsartan in *1b/*1b subjects tended to be lower than that in *1a/*1a subjects (73 % of *1a/*1a) and the AUC_{0-24} in *1b/*15 subjects was significantly lower than that in *1a/*15 subjects (67 % of *1a/*15) (Fig. II-5C, Table. II-1), exhibiting the similar trend as pravastatin. The renal clearance (CL_r) was almost the same in each haplotype group (Table. II-1).

Effect of OATP1B1 haplotype on the pharmacokinetics of temocapril and temocaprilat

After oral administration of temocapril, temocapril was rapidly eliminated from the blood and the concentration of temocapril was undetectable at 1 - 2 hr

after administration due to the rapid conversion of temocapril to the active metabolite, temocaprilat by carboxyl esterase (Fig. II-7A, B). Then, temocaprilat was detected at 0.25 hr and its plasma concentration reached a maximum at 0.75 - 2 hr after intake of temocapril (Fig. II-7A, B). The plasma concentration of temocaprilat showed a similar pattern in subjects with OATP1B1*1b/*1b and *1a/*1a (Fig. 3A), and *1b/*15 and *1a/*15 (Fig. II-6B). The mean AUC_{0-24} of temocaprilat in *1b/*1b subjects was not significantly very different from that in *1a/*1a subjects (87 % of *1a/*1a) and the AUC_{0-24} in *1b/*15 subjects was also not different from that in *1a/*15 subjects (91% of *1a/*15) (Fig. II-6C, Table. II-1). The OATP1B1*15 allele did not affect the AUC_{0-24} of temocaprilat. The renal clearance (CL_r) of temocaprilat was almost the same in each haplotype group (Table. II-1). On the other hand, the plasma concentration of temocapril in subjects with OATP1B1*1b/*1b tended to be lower than that in subjects with OATP1B1*1a/*1a (Fig. II-7A) and the plasma concentration in *1b/*15 subjects tended to be lower than that in *1a/*15 subjects (Fig. II-7B). Although not statistically significant, the AUC_{0-24} of temocapril in *1b/*1b carriers was lower than that in *1a/*1a carriers (67% of *1a/*1a) and the AUC_{0-24} in *1b/*15 carriers was lower than that in *1a/*15

carriers (86% of *1a/*15) (Fig. II-7C, Table. II-1), while the renal clearance (CL_r) of temocapril in each haplotype group was not significantly different (Table. II-1).

Correlation between the plasma AUC of pravastatin, valsartan, temocaprilat and temocapril in each subject

The plasma AUC values of valsartan in each subject were significantly correlated with those of pravastatin (Correlation coefficient: 0.630; $P < 0.01$) (Fig. II-8A). The AUC values of temocapril in each subject were also significantly correlated with those of pravastatin (Correlation coefficient: 0.602; $P < 0.01$) (Fig. II-8C). However, the AUC values of temocaprilat were not significantly correlated with those of pravastatin (Correlation coefficient: 0.229) (Fig. II-8B).

OATP1B1-mediated uptake of valsartan and temocaprilat in expression system.

The time-dependent uptake of valsartan and temocaprilat in OATP1B1-expressing HEK293 cells was significantly higher than that in vector-transfected control cells (Fig. II-9).

OATP1B1/MRP2-mediated transcellular of temocapril and RMS-416 in

OATP1B1/MRP2 double transfected MDCKII cells.

As a positive control, we checked that the vectorial basal-to-apical transcellular transport of estradiol-17β-glucuronide (OATP1B1/MRP2 bisubstrate) was clearly observed in OATP1B1/MRP2 double transfected cells (Fig. II-10C), while symmetrical transport was observed in OATP1B1 single transfected cells and vector-transfected control cells (Fig. II-10A, B) as shown in the previous report(Sasaki et al., 2002). Under the same condition, basal-to-apical transport of temocapril and RMS-416 was significantly larger than that in the opposite direction in OATP1B1/MRP2 double transfected cells (Fig. II-10F, I), whereas their vectorial transport was not observed in OATP1B1 single transfected cells (Fig. II-10E, H) and vector-transfected control cells (Fig. II-10D, G).

Discussion

We investigated the impact of the OATP1B1 haplotype, especially *1b, on the pharmacokinetics of three anionic drugs, pravastatin, valsartan and temocaprilat, in healthy volunteers. We also investigated whether the pharmacokinetics of each drug was correlated with other drugs in each subject.

Pravastatin, valsartan and temocaprilat are mainly excreted into bile without extensive metabolism and the involvement of transporters is needed to explain their efficient accumulation in liver. Considering the pharmacokinetic theory, assuming that the total clearance is accounted for by hepatic clearance, the plasma AUC after oral administration of drugs (AUC_{oral}) can be expressed by Eq. II-1:

$$AUC_{oral} = \frac{F \cdot Dose}{f_B \cdot CL_{\text{int}}} \qquad \text{(Eq. II-1)}$$

where F is the fraction of the dose absorbed into and through the gastrointestinal membranes, f_B is the blood unbound fraction and CL_{int} is the hepatic intrinsic clearance. Also, CL_{int} can be expressed as Eq. II-2(Shitara et al., 2005) :

$$CL_{\text{int}} = CL_{uptake} \times \frac{CL_{ex} + CL_{metab}}{CL_{ex} + CL_{metab} + CL_{eff}} \qquad \text{(Eq. II-2)}$$

where CL_{uptake}, CL_{ex}, CL_{metab} and CL_{eff} represent the intrinsic clearances for

hepatic uptake, biliary excretion, metabolism and sinusoidal efflux, respectively. Considering Eqs. II-1 and II-2, CL_{uptake} directly affects the plasma AUC after oral administration in any situation.

We especially focused on the impact of the OATP1B1*1b allele on the pharmacokinetics of the three drugs. The allele frequency of OATP1B1*1b is relatively high in some ethnic groups; 0.30 for European Americans, 0.74 for African Americans, and 0.63 for Japanese(Tirona et al., 2001; Nishizato et al., 2003).

Pravastatin has been reported to be a substrate of OATP1B1(Hsiang et al., 1999; Nakai et al., 2001; Sasaki et al., 2002; Kameyama et al., 2005). We demonstrated that valsartan and temocaprilat could also be recognized by OATP1B1 as a substrate (Fig. II-9).

The OATP1B1*1b allele significantly reduced the plasma AUC of pravastatin compared with *1a, which is consistent with a previous report(Mwinyi et al., 2004). The renal clearance of pravastatin was not affected by *1b, suggesting that the OATP1B1*1b variant apparently enhances the hepatic uptake activity of pravastatin. On the other hand, the OATP1B1*15 allele did not remarkably affect the plasma AUC of pravastatin in the present study, which apparently

differs from earlier reports showing that the *15 allele results in a significant increase in the plasma AUC of pravastatin(Nishizato et al., 2003; Niemi et al., 2004). After oral administration, a significant amount of pravastatin was converted to RMS-416 (3' α-isopravastatin) mainly in the stomach by chemical reaction rather than by enzymatic metabolism because pravastatin is unstable in acidic solution(Triscari et al., 1995) (Fig. II-2A). In the present study, the inter-individual difference in the plasma AUC of RMS-416 was about fifty-fold (2.37 – 120 ng*hr/mL; average = 48.8 ng*hr/mL). It is generally accepted that the pH values in the stomach exhibit large inter-individual differences. We hypothesized that this difference might affect the conversion rate to RMS-416, which could mask the effect of OATP1B1*15 on the pharmacokinetics of pravastatin in our cases. RMS-416 is an epimer of pravastatin and only the position of one hydroxyl group was different. We confirmed that RMS-416 is also a substrate of OATP1B1 (Fig. II-10). Assuming that the pharmacokinetic profile of pravastatin was not so much different from that of RMS-416 due to their similar chemical structures, a genetic polymorphism of OATP1B1 would affect the pharmacokinetics of the sum of pravastatin and RMS-416 more markedly than that of pravastatin itself. In the present study, we could see the expected

tendency showing that the *1b allele reduced the plasma AUC of the sum of pravastatin and RMS-416 compared with *1a, whereas the *15 allele increased the plasma AUC (Table II-1). Recent studies have demonstrated that the Val174Ala mutation in OATP1B1 could alter the cholesterol lowering effect of pravastatin(Tachibana-Iimori et al., 2004; Niemi et al., 2005c). Because RMS-416 is not pharmacologically active, our study suggests that the conversion rate to RMS-416 as well as the genetic polymorphism in OATP1B1 may have an effect on the pharmacokinetics and pharmacological action of pravastatin.

In the case of valsartan, the *1b allele showed a reduction in the plasma AUC of valsartan, but the *15 allele did not show any increase in the plasma AUC, which is almost the same as pravastatin. Unfortunately, the difference in its AUC between *1a and *1b didn't show statistical significance probably due to the lack of statistical power and we think that additional number of subjects will be needed to show the significant difference. Valsartan was partly metabolized to the 4-hydroxylated form (M-2) by CYP2C9(Waldmeier et al., 1997), but a previous report indicated that, after oral administration of [^{14}C]-valsartan, this metabolite accounted for only 10 % of the total radioactivity in feces and

urine(Waldmeier et al., 1997). Therefore, the interindividual difference in CYP2C9 activity plays only a minor role in the pharmacokinetics of valsartan. The solubility of valsartan is drastically affected by the pH and it is possible that an interindividual difference in the pH value in the gastrointestinal tract may affect its solubility and the subsequent amount of valsartan absorbed(Criscione et al., 1995). However, one report demonstrated that coadministration of cimetidine increased the plasma AUC only by 7 %(Schmidt et al., 1998). So, the exact reason why the *15 allele did not affect the pharmacokinetics of valsartan remains to be clarified.

The plasma AUC of temocapril and temocaprilat was not changed significantly in each haplotype group. However, there was a trend suggesting that the *1b allele reduced the plasma AUC of temocapril and temocaprilat and that the *15 allele showed a slight increase in the plasma AUC. We checked that temocapril is also a substrate of OATP1B1 (Fig. II-10). The difference in the plasma AUC of temocaprilat in each haplotype group was relatively small compared with other drugs.

We also compared the pharmacokinetics of the three drugs in each subject and the plasma AUC of pravastatin was significantly correlated with that of

valsartan and temocapril, but not temocaprilat (Fig. II-8). This result suggested that the clearance mechanism of pravastatin may share with that of valsartan and temocapril, and that the relative contribution of OATP1B1 to the hepatic uptake of pravastatin may be similar to that of valsartan and temocapril, but be larger than that of temocaprilat.

Some *in vitro* studies have indicated that the transport activity of several compounds including pravastatin in the OATP1B1*1b variant was almost comparable with that of OATP1B1*1a(Tirona et al., 2001; Iwai et al., 2004; Kameyama et al., 2005; Nozawa et al., 2005). However, this study demonstrated that subjects with OATP1B1*1b showed an increase in the hepatic clearance compared with those with OATP1B1*1a. We hypothesized that this apparent discrepancy may be explained by the higher expression level of OATP1B1*1b in the liver compared with that of OATP1B1*1a. This can be proven by investigating the relative expression level of OATP1B1*1a and *1b in several batches of human hepatocytes which are genotyped in advance. Moreover, we must pay attention to several pharmacokinetic issues such as the different proportion of hepatic clearance to total clearance, the different contribution of OATP1B1 to the overall hepatic uptake, and the substrate

specificity of the effect of genetic polymorphisms in OATP1B1. The percentage of hepatic clearance with regard to the total clearance has been estimated to be about 53 % for pravastatin, 71 % for valsartan and 62 % for temocaprilat in humans(Singhvi et al., 1990; Waldmeier et al., 1997) (temocaprilat: drug information published by Sankyo Co., Ltd.). Previous reports suggest that the de-esterification of temocapril mainly occurs in liver (drug information published by Sankyo Co., Ltd.). The urinary excreted temocapril as a percentage of the administered dose is about 1.1 % in this study. We think it is possible that temocapril is efficiently taken up into hepatocytes followed by conversion to temocaprilat and its hepatic clearance is much higher than the renal clearance. That may be the reason why the AUC of temocapril showed better correlation with that of pravastatin than temocaprilat. Regarding the contribution of individual transporters, our preliminary study suggested that all three compounds are substrates of OATP1B3 as well as OATP1B1 (Hirano et al., unpublished observations). The previous studies suggested that pravastatin is thought to be mainly taken up via OATP1B1(Nakai et al., 2001). From the result of the present study, we speculated that the relative importance of OATP1B1 in the hepatic clearance is in the order of pravastatin > valsartan,

temocapril > temocaprilat. We have established the methodology for estimating the contribution of OATP1B1 and OATP1B3 to the overall hepatic uptake by using expression systems and human hepatocytes(Hirano et al., 2004). Taking this information into consideration, the prediction of the effect of genetic polymorphisms in OATP1B1 on the pharmacokinetics of drugs from in vitro data will be the subject of further investigation. And very recently, Zhang et al. have demonstrated that SNP (Q141K) in BCRP, an efflux transporter, affected the pharmacokinetics of rosuvastatin(Zhang et al., 2006b). Regardless of the situations, we showed that apparent intrinsic hepatotic clearance is directly proportional to the intrinsic uptake clearance which is sometimes governed by uptake transporters like OATP1B1. However, this doesn't mean that efflux transporters cannot determine the overall hepatic clearance and we will also need to investigate the effect of the SNPs in efflux transporters on the pharmacokinetics of drugs.

In conclusion, our study indicated that the OATP1B1*1b allele increases the hepatic clearance of pravastatin compared with the *1a allele and valsartan and temocapril showed the similar tendency as the case of pravastatin. And the plasma AUC of pravastatin correlates well with that of valsartan and temocapril,

suggesting that pravastatin, valsartan and temocapril may share the same elimination pathway.

Tables and figures

		*1a/*1a	*1b/*1b	*1a/*15	*1b/*15
number of subjects		5	7	6	5
<pravastatin>					
AUC_{0-24}	(ng*hr/mL)	73.2 ± 23.5	47.4 ± 19.9*1	69.2 ± 23.4	38.2 ± 15.9*2
CL_r	(L/hr)	15.1 ± 2.7	18.6 ± 7.6	12.6 ± 2.5	17.0 ± 3.5
<pravastatin+RMS-416>					
AUC_{0-24}	(ng*hr/mL)	112 ± 25	76.1 ± 20.4	143 ± 40	95.1 ± 33.6*2
CL_r	(L/hr)	12.5 ± 2.0	16.0 ± 8.5	11.0 ± 1.5	13.5 ± 2.4
<valsartan>					
AUC_{0-24}	(μg*hr/mL)	12.3 ± 4.6	9.01 ± 3.33	9.40 ± 4.34	6.31 ± 3.64
CL_r	(L/hr)	0.450 ± 0.063	0.482 ± 0.049	0.489 ± 0.109	0.477 ± 0.096
<temocaprilat>					
AUC_{0-24}	(ng*hr/mL)	426 ± 91	371 ± 100	429 ± 41	389 ± 77
CL_r	(L/hr)	1.41 ± 0.06	1.29 ± 0.26	1.31 ± 0.12	1.32 ± 0.15
<temocapril>					
AUC_{0-24}	(ng*hr/mL)	18.5 ± 7.7	12.4 ± 4.1	19.0 ± 4.1	16.4 ± 5.0
CL_r	(L/hr)	0.818 ± 0.476	1.82 ± 1.16	1.21 ± 0.52	2.14 ± 1.77

Table. II-1 Plasma AUC and renal clearance of pravastatin and its metabolite (RMS-416), valsartan, and temocapril and its active metabolite (temocaprilat) in each haplotype group

AUC_{0-24}, the area under the plasma concentration-time curve from time 0 to 24 hours; CL_r, renal clearance. Each value represents the mean ± S.D.

*1: significantly different from values in *1a/*1a subjects as determined by ANOVA with Fisher's least significant difference test ($P < 0.05$).

*2: significantly different from values in *1a/*15 subjects as determined by ANOVA with Fisher's least significant difference test ($P < 0.05$).

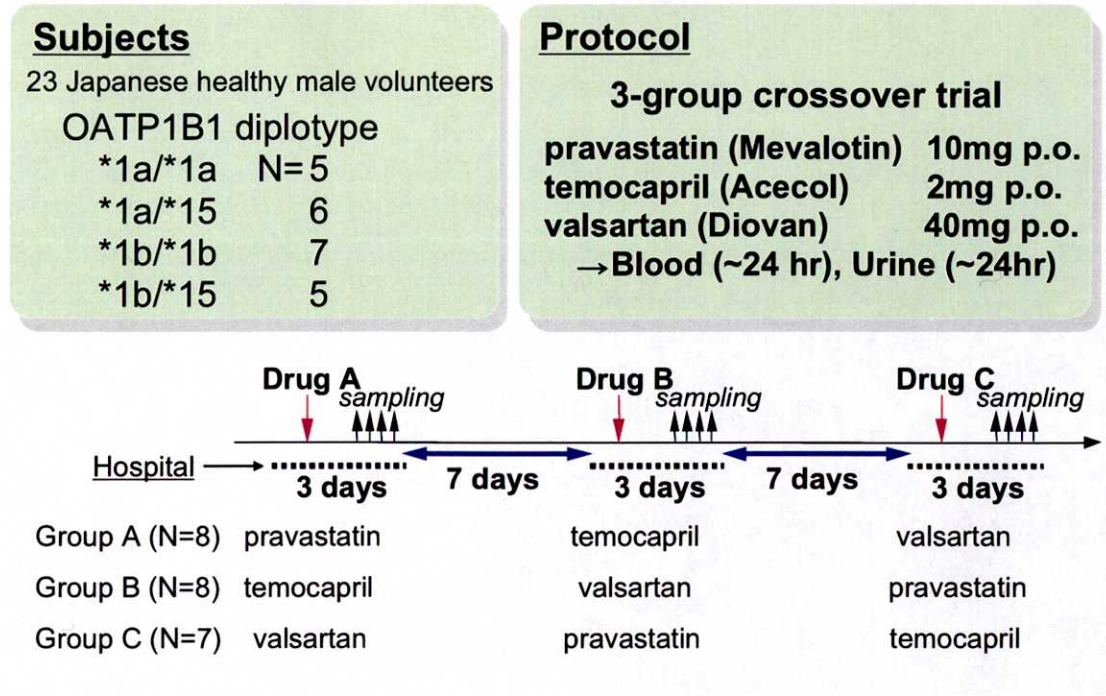

Fig. II-1 Schematic diagram of the protocol of clinical study

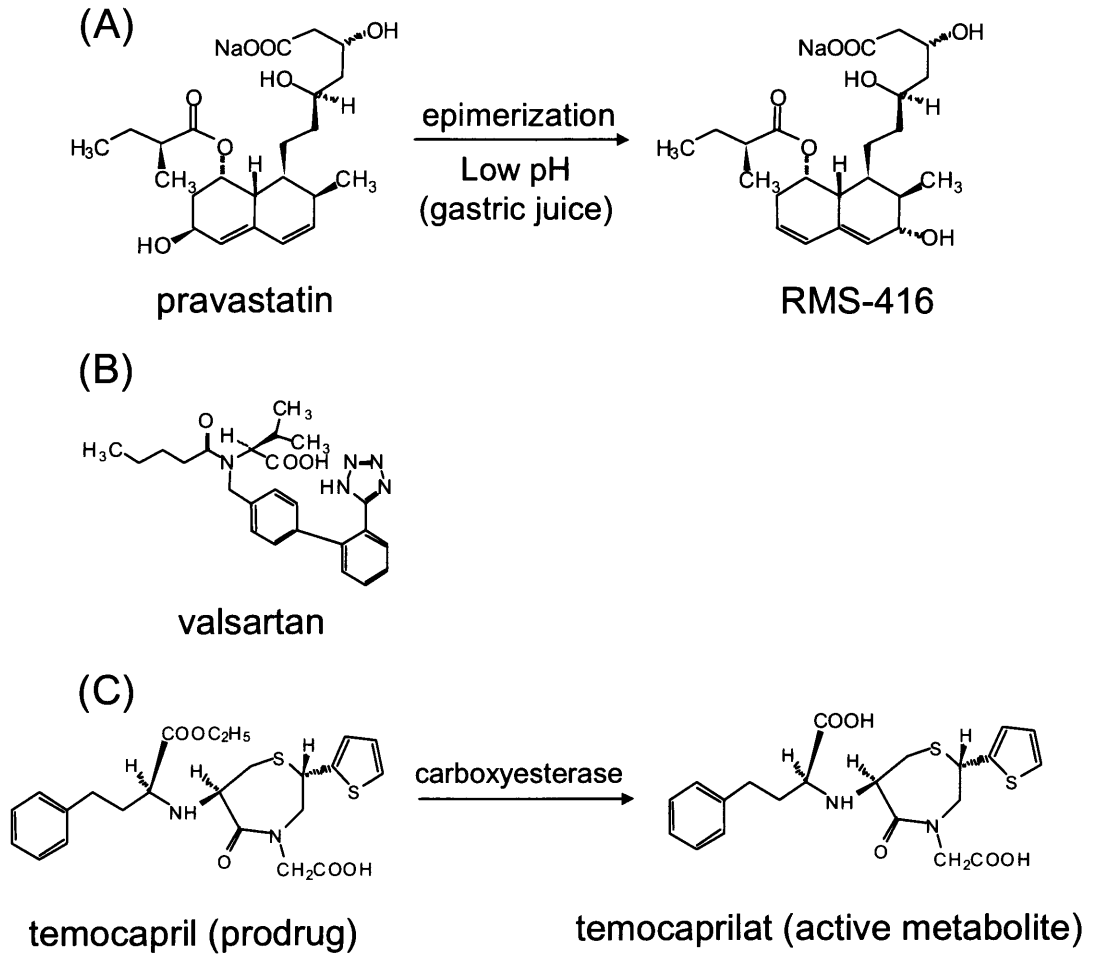

Fig. II-2 Chemical structures of drugs and their metabolites used in the clinical study

(A) Pravastatin is converted to its epimer, RMS-416 by non-enzymatic reaction under low pH condition.

(C) Temocapril is a prodrug and it is rapidly converted to temocaprilat, an active metabolite, by carboxyesterase.

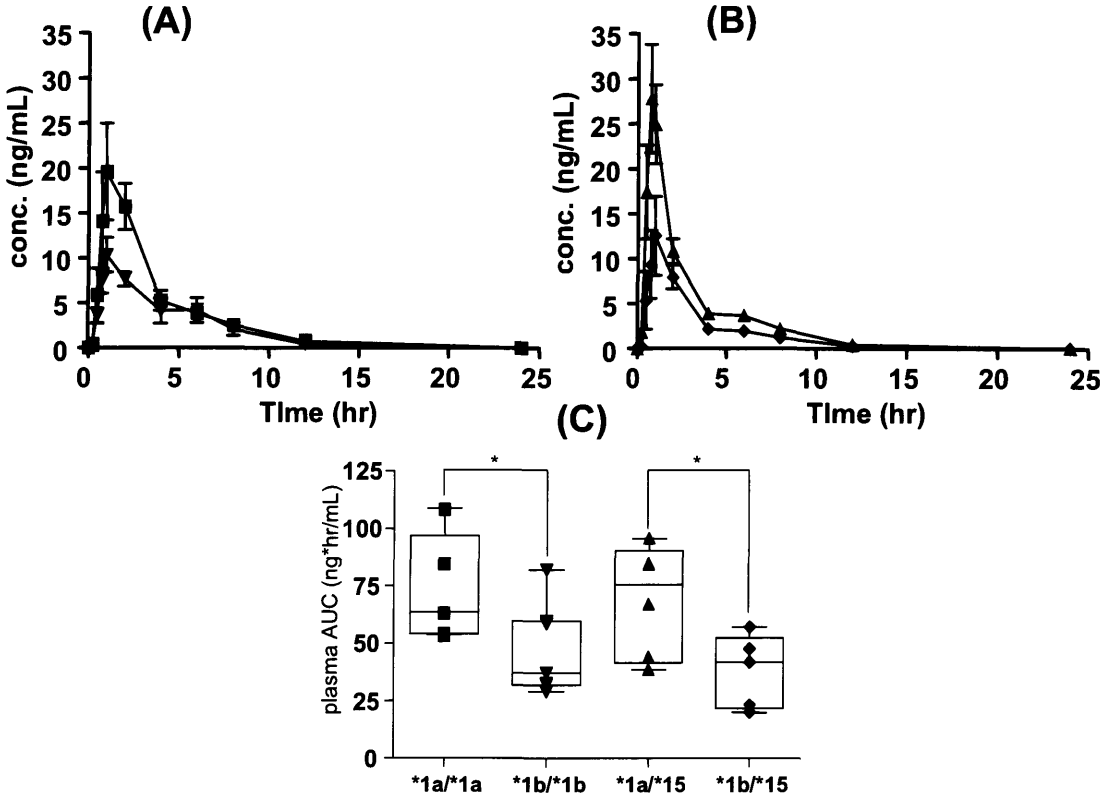

Fig. II-3 Effect of OATP1B1 haplotype on the pharmacokinetics of pravastatin

(A) Plasma concentration-time profiles of pravastatin after oral administration of 10 mg of pravastatin in subjects with OATP1B1*1a/*1a (square; n=5) and *1b/*1b (inverted triangle; n=7). Each point represents mean ± S.D.
(B) Plasma concentration-time profiles of pravastatin after oral administration of 10 mg pravastatin in subjects with OATP1B1*1a/*15 (triangle; n=6) and *1b/*15 (diamond; n=5). Each point represents mean ± S.D.
(C) Box-whisker plot of the plasma AUC of pravastatin in each haplotype group. The horizontal line within each box represents the median. The box edges represent the lower (25th) and upper (75th) quartiles, respectively. The whiskers extend from the lower and upper quartiles to the furthest data points still within a distance of 1.5 interquartile ranges from the lower and upper quartiles. Individual data points were overlaid on the box-whisker plot. *: statistically significant difference shown by ANOVA with Fisher's least significant difference test ($P < 0.05$)

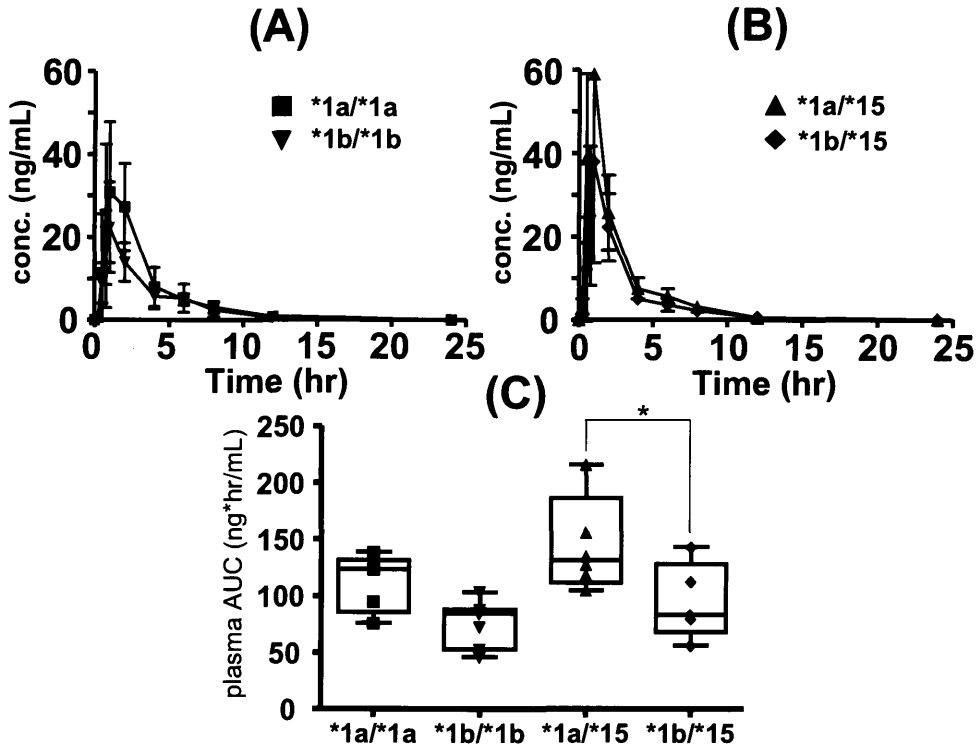

Fig. II-4 Effect of OATP1B1 haplotype on the pharmacokinetics of the sum of pravastatin and RMS-416 (major metabolite)

(A) Plasma concentration-time profiles of the sum of pravastatin and RMS-416 after oral administration of 10 mg of pravastatin in subjects with OATP1B1*1a/*1a (square; n=5) and *1b/*1b (inverted triangle; n=7). Each point represents mean ± S.D.
(B) Plasma concentration-time profiles of the sum of pravastatin and RMS-416 after oral administration of 10 mg pravastatin in subjects with OATP1B1*1a/*15 (triangle; n=6) and *1b/*15 (diamond; n=5). Each point represents mean ± S.D.
(C) Box-whisker plot of the plasma AUC of the sum of pravastatin and RMS-416 in each haplotype group. The horizontal line within each box represents the median. The box edges represent the lower (25th) and upper (75th) quartiles, respectively. The whiskers extend from the lower and upper quartiles to the furthest data points still within a distance of 1.5 interquartile ranges from the lower and upper quartiles. Individual data points were overlaid on the box-whisker plot. *: statistically significant difference shown by ANOVA with Fisher's least significant difference test ($P < 0.05$)

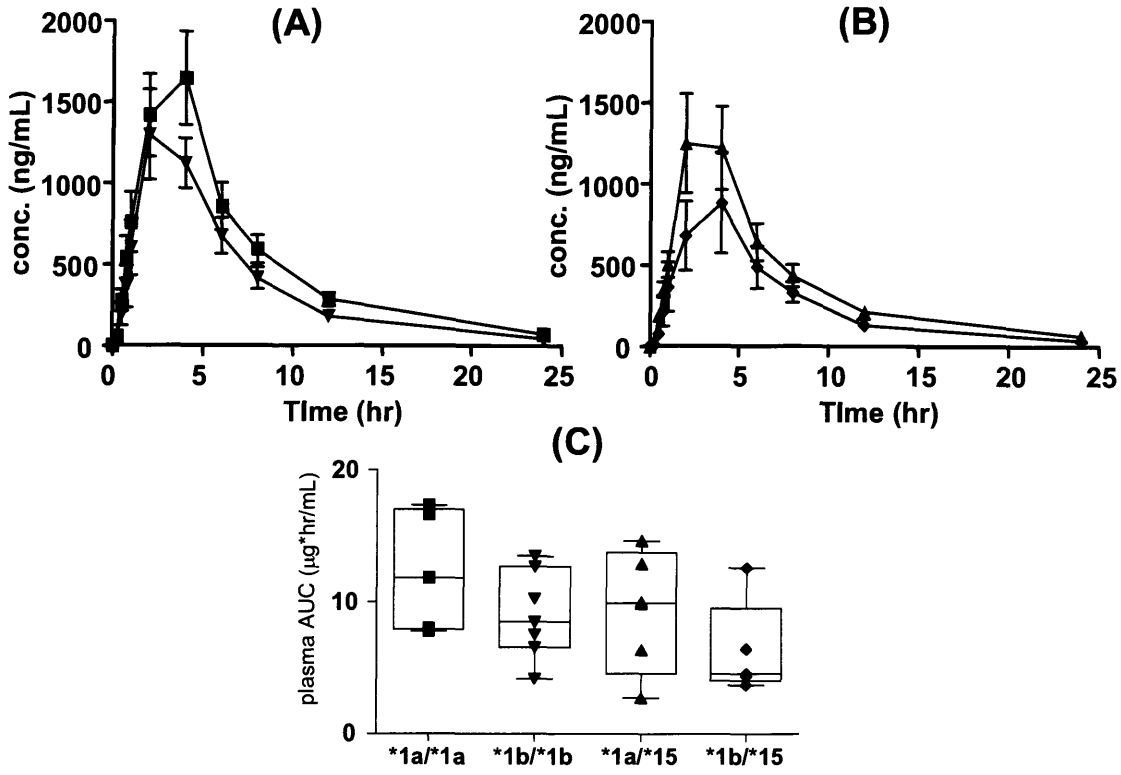

Fig. II-5 Effect of OATP1B1 haplotype on the pharmacokinetics of valsartan

(A) Plasma concentration-time profiles of valsartan after oral administration of 40 mg valsartan in subjects with OATP1B1*1a/*1a (square; n=5) and *1b/*1b (inverted triangle; n=7). Each point represents mean ± S.D.

(B) Plasma concentration-time profiles of valsartan after oral administration of 40 mg valsartan in subjects with OATP1B1*1a/*15 (triangle; n=6) and *1b/*15 (diamond; n=5). Each point represents mean ± S.D.

(C) Box-whisker plot of the plasma AUC of valsartan in each haplotype group. The horizontal line within each box represents the median. The box edges represent the lower (25th) and upper (75th) quartiles, respectively. The whiskers extend from the lower and upper quartiles to the furthest data points still within a distance of 1.5 interquartile ranges from the lower and upper quartiles. Individual data points were overlaid on the box-whisker plot.

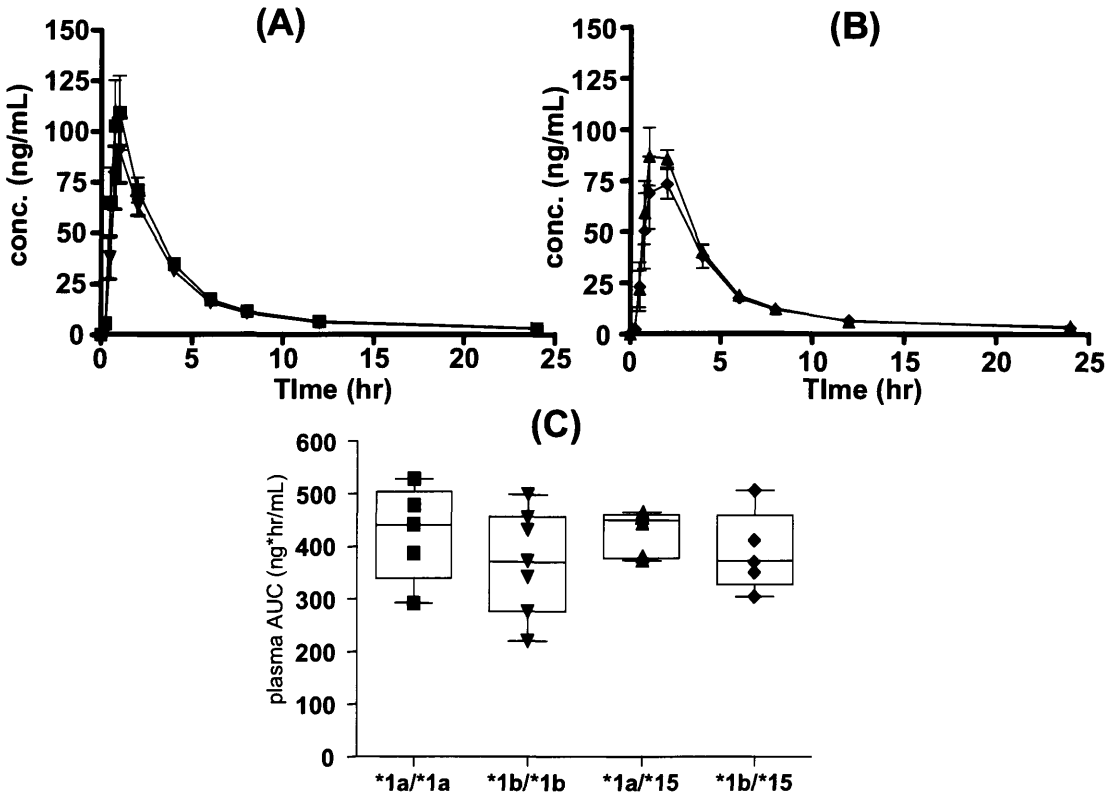

Fig. II-6 Effect of OATP1B1 haplotype on the pharmacokinetics of temocaprilat

(A) Plasma concentration-time profiles of temocaprilat after oral administration of 2 mg temocapril in subjects with OATP1B1*1a/*1a (square; n=5) and *1b/*1b (inverted triangle; n=7). Each point represents mean ± S.D.
(B) Plasma concentration-time profiles of temocaprilat after oral administration of 2 mg temocapril in subjects with OATP1B1*1a/*15 (triangle; n=6) and *1b/*15 (diamond; n=5). Each point represents mean ± S.D.
(C) Box-whisker plot of the plasma AUC of temocaprilat in each haplotype group. The horizontal line within each box represents the median. The box edges represent the lower (25th) and upper (75th) quartiles, respectively. The whiskers extend from the lower and upper quartiles to the furthest data points still within a distance of 1.5 interquartile ranges from the lower and upper quartiles. Individual data points were overlaid on the box-whisker plot.

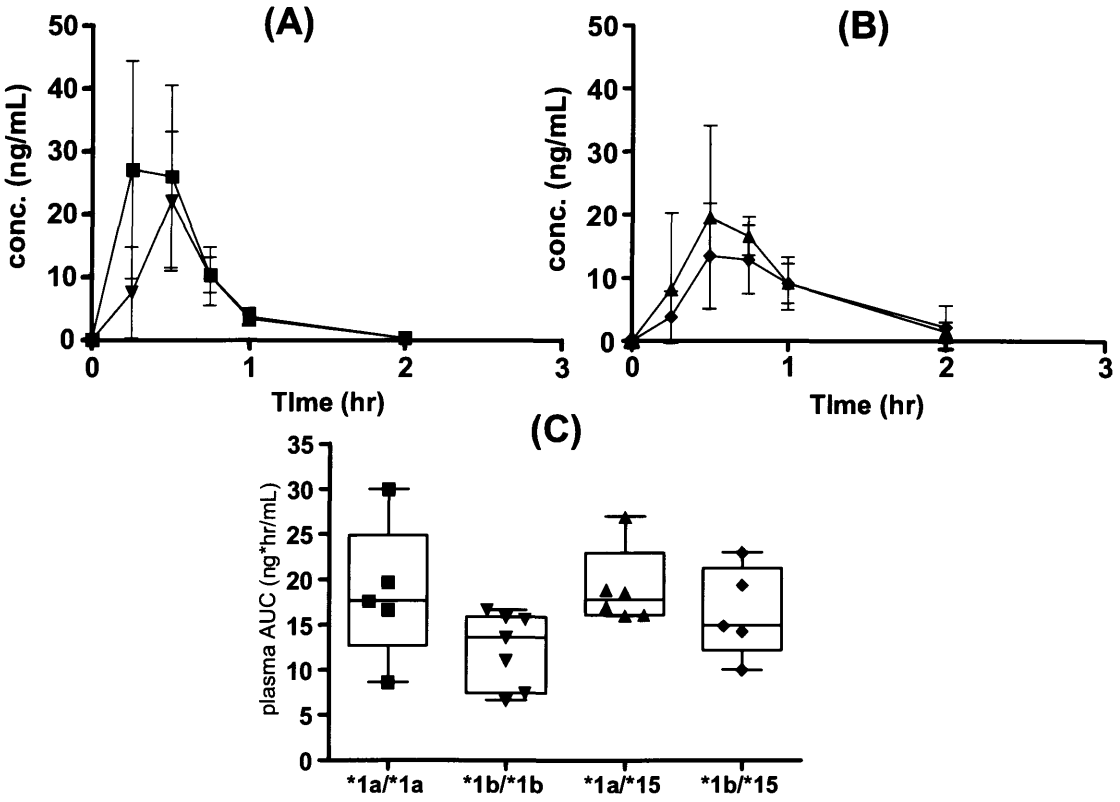

Fig. II-7 Effect of OATP1B1 haplotype on the pharmacokinetics of temocapril

(A) Plasma concentration-time profiles of temocapril after oral administration of 2 mg temocapril in subjects with OATP1B1*1a/*1a (square; n=5) and *1b/*1b (inverted triangle; n=7). Each point represents mean ± S.D.
(B) Plasma concentration-time profiles of temocapril after oral administration of 2 mg temocapril in subjects with OATP1B1*1a/*15 (triangle; n=6) and *1b/*15 (diamond; n=5). Each point represents mean ± S.D.
(C) Box-whisker plot of the plasma AUC of temocapril in each haplotype group. The horizontal line within each box represents the median. The box edges represent the lower (25th) and upper (75th) quartiles, respectively. The whiskers extend from the lower and upper quartiles to the furthest data points still within a distance of 1.5 interquartile ranges from the lower and upper quartiles. Individual data points were overlaid on the box-whisker plot.

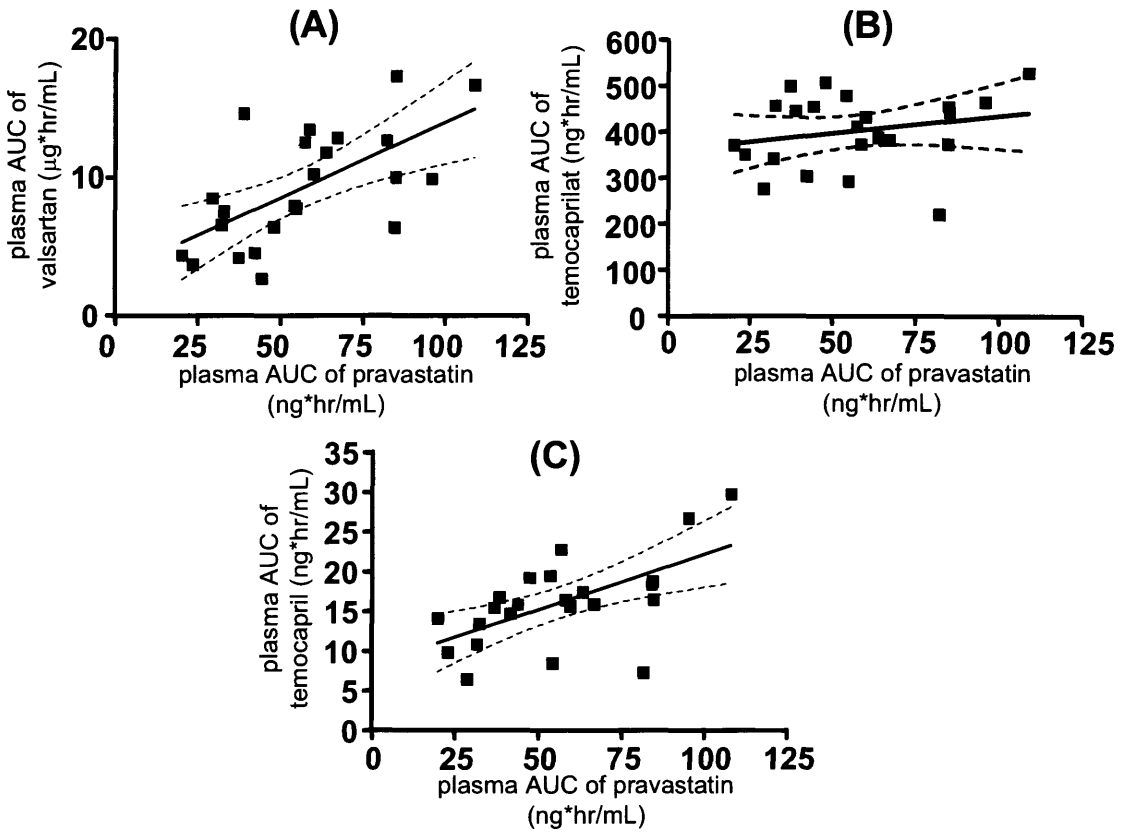

Fig. II-8 Correlation between the plasma AUC of pravastatin and valsartan (A), the plasma AUC of pravastatin and temocaprilat (B), and the plasma AUC of pravastatin and temocapril (C).

Each point represents the data for each subject. The solid line represents the fitted line calculated by linear regression analysis and the dotted line represents the 95 % confidence intervals of the correlation.

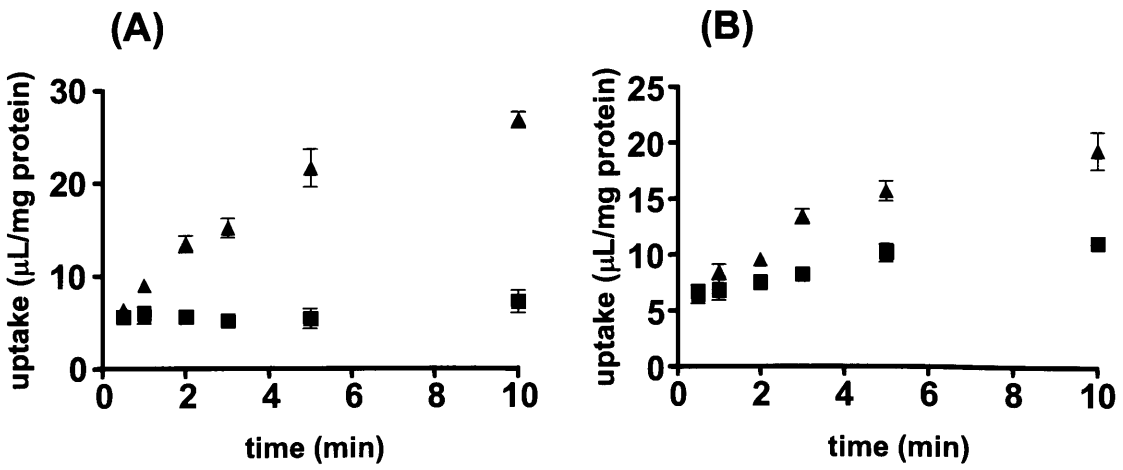

Fig. II-9 Time-dependent uptake of valsartan (A) and temocaprilat (B) in OATP1B1-expressing cells and control cells.

The uptake of valsartan (A) and temocaprilat (B) by OATP1B1-transfected HEK293 cells was examined at 37 °C. Triangles and squares represent the uptake by OATP1B1- and vector-transfected cells, respectively. Each point represents the mean ± S.E. (n=3).

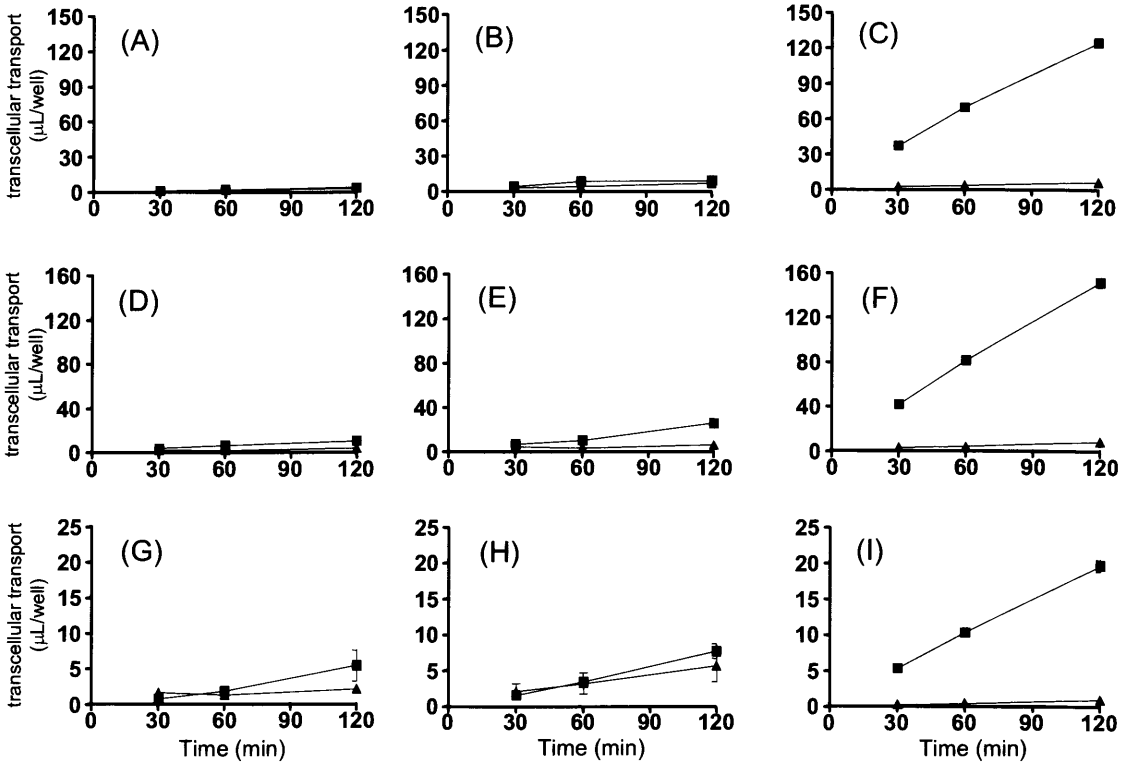

Fig. II-10 Time profiles for the transcellular transport of estradiol-17β-glucuronide (A,B,C), temocapril (D,E,F) and RMS-416 (G,H,I) across MDCKII monolayers.

Transcellular transport of estradiol-17β-glucuronide (1 μM), temocapril (1 μM) and RMS-416 (10 μM) across MDCKII monolayers expressing OATP1B1 (B,E,H) and both OATP1B1 and MRP2 (C,F,I) was compared with that across the control MDCKII monolayer (A,D,G). Triangles and squares represent the transcellular transport in the apical-to-basal and basal-to-apical direction, respectively. Each point and vertical bar represents the mean ± S.E. of three determinations. Where vertical bars are not shown, the S.E. was contained within the limits of the symbol.

Conclusion and future perspectives

In Part I, we investigated the importance of uptake transporters in the hepatic transport of ursodeoxycholate (UDCA) and its conjugates by using human cryopreserved hepatocytes and transporter expression systems. As a result, we have shown that UDCA and its conjugates are taken up into human hepatocytes via both Na^+-dependent and Na^+-independent pathways and the relative contribution of the Na^+-independent uptake of the glycoursodeoxycholate (GUDC), a major metabolite of UDCA in humans, to the overall hepatic uptake in human hepatocytes is greater than that of UDCA and tauroursodeoxycholate (TUDC). We also showed that GUDC and TUDC can be recognized by NTCP, OATP1B1 and OATP1B3. It is generally believed that the hepatic uptake of bile acids is mainly mediated by NTCP. In this case, after oral administration of UDCA, it is mainly conjugated with glycine in humans and GUDC is the major molecular form which undergoes enterohepatic circulation. These results suggest that OATP1B1 and OATP1B3 as well as NTCP can be determinant factors for the clinical pharmacokinetics and subsequent pharmacological effects of UDCA, although UDCA is a bile acid. We have now started a clinical study investigating the effect of genetic polymorphisms of

OATP1B1 on the pharmacokinetics of UDCA and its conjugates and glycyrrhizin, which is also frequently used for the treatment of hepatic diseases, in patients with chronic hepatitis C. As mentioned previously, the enterohepatic circulation of UDCA and its conjugates is dominated by not only hepatic uptake transporters (OATPs, NTCP) but also by other transporters involved in biliary excretion and intestinal absorption. Moreover, because the relative contribution of uptake transporters to the overall membrane transport of UDCA and its conjugates is different, and this may be true for other transport process, the function of conjugation enzymes may also affect the pharmacokinetics of UDCA and its conjugates. Therefore, we also need to investigate the involvement of other transporters in their hepatobiliary transport and the relative importance of transporters and enzymes in their pharmacokinetics.

Cryopreserved human hepatocytes have enabled us to predict the quantitative contribution of each transporter and metabolic enzyme to the overall hepatic uptake and metabolism of drugs(Hengstler et al., 2000; Shitara et al., 2003b). We can also use several kinds of knockout animals to directly show the role of specific genes in the *in vivo* plasma concentration profiles and tissue distribution of drugs. However, species differences in transport function have been

observed(Dietrich et al., 2001; van Herwaarden et al., 2003) and, especially in the case of metabolic enzymes and OATP family transporters, so that we cannot identify the exact genes in humans corresponding to those in rodents(Zuber et al., 2002; Hagenbuch and Meier, 2003). Moreover, we need to keep in mind that, in some cases, there is a compensatory change in the expression level of other genes. For example, in Eisai hyperbilirubinemic rats (EHBR) whose Mrp2 is hereditary deficient, Mrp3 located on the sinusoidal membrane is up-regulated, and this might confound the effect of specific genes on the pharmacokinetics of drugs(Ogawa et al., 2000). Several useful techniques for knockdown of specific genes, such as ribozyme and RNA interference (RNAi), have been developed. However, it is difficult to apply these techniques in our research because the long-term culture of hepatocytes itself dramatically reduces the expression levels of several kinds of transporters and metabolic enzymes(Ishigami et al., 1995; Rippin et al., 2001). Therefore, we established three methods using (1) transporter-specific substrate (RAF method), (2) transporter-specific inhibitor and (3) Western blot analysis for estimating the contribution of each transporter to drug uptake(Hirano et al., 2004; Hirano et al., 2006; Ishiguro et al., 2006). Of course, we understand that each method has

both advantages and disadvantages, and so we recommend that users compare the results obtained from different approaches and validate the results. We have recently investigated several kinds of anionic drugs, such as angiotensin II receptor antagonists, fexofenadine (H1-antagonist), and pitavastatin (HMG-CoA reductase inhibitor), and the relative importance of OATP1B1 and OATP1B3 for their hepatic uptake differs from drug to drug(Hirano et al., 2004; Shimizu et al., 2005; Ishiguro et al., 2006; Yamashiro et al., 2006). I believe that our methods are very simple and suitable for the high throughput screening used in drug development. Cryopreserved human hepatocytes can be easily purchased from some distributors in Japan, but they are very expensive and there are large inter-batch differences in the function of transporters. In our experience, only about 30-40 % of the available batches of hepatocytes exhibit enough transport activity and we cannot simply say that the large inter-batch difference is explained by the intrinsic inter-individual variability of the transport function because differences in the conditions of the preparation of human hepatocytes also affect the variation(Shitara et al., 2003b). Human hepatocytes derived from embryonic stem (ES) cells or multipotent precursor cells with their detoxification system intact are now under development(Ishii et al., 2005). If

these cell lines can be stably supplied, they will be widely used to predict the function of transporters and metabolic enzymes in human liver. We will also need to develop culture systems for hepatocytes which can be easily used for drug screening with long-term retention of the expression of proteins for detoxification of xenobiotics. Some groups have reported that a collagen-sandwich culture system can maintain the expression of several kinds of transporters in hepatocytes at the same level as that in intact hepatocytes for one week(Hoffmaster et al., 2004). Moreover, hepatocytes cultured in this system are efficiently polarized and form the bile canalicular pocket between the cells so that we can measure the amount of ligands excreted into the bile pocket by treatment with Ca^{+}-free buffer which can destroy the tight junction(Hoffmaster et al., 2004). Also, this system is very useful for evaluating the biliary excretion of ligands *in vitro*. Bi et al. have demonstrated that this culture system can be applied to cryopreserved human hepatocytes(Bi et al., 2006) and Tian et al. have succeeded in the knockdown of drug transporters, Mrp2 and Mrp3, in sandwich-cultured rat hepatocytes by using small interfering RNA (siRNA)(Tian et al., 2004). As far as the prediction of the biliary excretion of drugs in humans is concerned, we have established double transfected cell lines which express

both uptake and efflux transporters(Sasaki et al., 2002; Sasaki et al., 2004; Matsushima et al., 2005). If a compound is a bisubstrate of uptake and efflux transporters, the basal-to-apical transcellular vectorial transport is significantly larger compared with that in the opposite direction when cells are seeded on a cell culture insert. By using these cell lines and sandwich-cultured hepatocytes, we can investigate the relative contribution of each efflux transporter to the overall biliary excretion of drugs.

In Part II, we performed a clinical study to investigate the importance of OATP1B1 in the pharmacokinetics of drugs in humans *in vivo*. Some groups have reported that single nucleotide polymorphisms (SNPs) in OATP1B1 affected the pharmacokinetics of pravastatin, which is thought to be mainly taken up into hepatocytes by OATP1B1(Nishizato et al., 2003; Mwinyi et al., 2004; Niemi et al., 2004). Although OATP1B1 can recognize many kinds of drugs used in clinical situations, few reports have shown that OATP1B1 SNPs can also affect the pharmacokinetics of the substrate drugs for OATP1B1 other than statins. As a result, we investigated the major clearance mechanism of pravastatin, valsartan and temocapril and found that it appears to be similar and the OATP1B1*1b allele can affect the clinical pharmacokinetics of pravastatin,

and, possibly, valsartan and temocapril. At the present, the pharmacokinetics of many drugs, such as atrasentan (endothelin antagonist), repaglinide and nateglinide (antidiabetic), fexofenadine (H1-antagonist), pitavastatin and rosuvastatin (HMG-CoA reductase inhibitor), can also be affected by the haplotype of OATP1B1(Chung et al., 2005; Lee et al., 2005; Niemi et al., 2005a; Katz et al., 2006; Zhang et al., 2006a). If we wish to predict the effect of SNPs in transporter on the pharmacokinetics of drugs, we must consider the following issues as described in Fig. C-1; (1) the change in the transport activity of drugs in cells expressing mutated transporter compared with wild type, (2) the contribution of target transporter to the overall hepatic uptake clearance, (3) the rate-determining process in the apparent intrinsic hepatic clearance, and (4) the effect of the change in apparent intrinsic clearance on the hepatic and total clearance of drugs. Iwai et al. have constructed recombinant cell lines expressing mutated OATP1B1 proteins which correspond to the major haplotypes in humans (OATP1B1*1a, *1b, *5, and *15) and characterized the functional change in the transport activity of compounds in each cell line(Iwai et al., 2004). Regarding the contribution, we have established methods for its estimation as described above(Hirano et al., 2004; Hirano et al., 2006; Ishiguro

et al., 2006). The information about (3) and (4) can be roughly estimated from *in vitro* and *in vivo* data, although it is difficult to estimate the backflux clearance from cells to blood from *in vitro* data and the *in vivo* biliary excretion clearance. Combining these data, we can predict the impact of genetic polymorphisms of transporters on the pharmacokinetics of drugs prior to conducting clinical studies. Another approach to the prediction of pharmacokinetics for individual subjects is the use of *in vivo* phenotyping to study the plasma concentration profiles of "probe drugs", which are ideally transporter-specific substrates in humans. In the field of metabolic enzymes, to know the intrinsic metabolic activities of each CYP enzymes, sets of specific substrates of CYP subtypes (so called "cocktail") have been developed(Tanaka et al., 2003). Cocktail drugs are administered to humans and their metabolites in plasma and urine were analyzed, then we can easily get the information on several CYP activities of individuals in a single experiment. Because we cannot directly measure the biliary excretion clearance in humans, probe drugs for transporters must be sensitive to changes in their plasma concentration when there is a functional change in the specific transporter. From the results of clinical studies, pravastatin may be used as a probe drug for OATP1B1(Nishizato et al., 2003; Mwinyi et al., 2004; Niemi et al.,

2004). Using positron emission tomography (PET) or single photon emission computed tomography (SPECT), we can obtain the time profile of the concentration of drugs in each tissue in humans(Sasongko et al., 2005; Lee et al., 2006). So, if we can synthesize radiolabeled probe drugs suitable for PET or SPECT, we can obtain detailed data on pharmacokinetics and tissue distribution directly in humans and, by combining these data and several kinds of *in vitro* data, we can construct more accurate pharmacokinetic models of drugs.

It is possible that the SNPs in transporters which affect the pharmacokinetics have the potential to change the subsequent pharmacological effects of drugs. Interestingly, Niemi et al. have shown that the acute cholesterol-lowering effect of pravastatin was influenced by the OATP1B1 haplotypes after a single oral administration of pravastatin(Niemi et al., 2005c). However, Igel et al. have shown that, after multiple dosing of pravastatin, the inter-individual variability in the pharmacological effect could not be explained by OATP1B1 haplotypes, although its pharmacokinetics was different among haplotype groups(Igel et al., 2006). Therefore, a change in the pharmacokinetics does not always produce a pharmacological effect. In order to predict a pharmacological effect, one suitable strategy is to construct an appropriate mathematical model of the

pharmacodynamics of pravastatin based on molecular mechanisms. I have named this model "focused systems biology", in which the minimum number of molecules which are necessary to understand the major pathway for the pharmacological effects are included. We will try to carry out such pharmacodynamic modeling and combine this model with physiologically-based pharmacokinetic models to predict the time profile of the effect of drugs.

In conclusion, through *in vitro* and *in vivo* studies, I have been able to show the importance of hepatic uptake transporters in the pharmacokinetics of several drugs selectively accumulated in liver. The clinical significance of the functional change in each transporter should be further investigated and the tools and methods for accurate prediction of the *in vivo* plasma concentrations and pharmacological effects of drugs from *in vitro* data will need to be developed as proposed above.

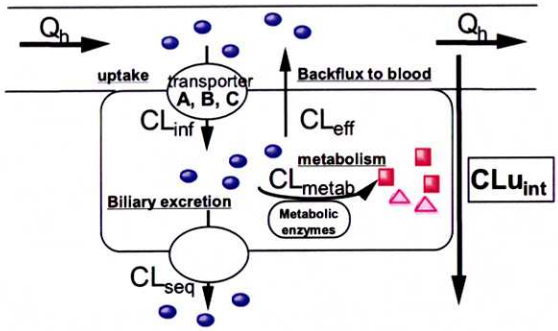

1) Contribution of each transporter to the membrane transport

$$CL_{inf} = CL_{inf,A} + CL_{inf,B} + CL_{inf,C} + \cdots$$

2) The rate-determining process in the apparent intrinsic hepatic clearance

$$CLu_{int} = CL_{inf} \times \frac{CL_{metab} + CL_{seq}}{(CL_{metab} + CL_{seq}) + CL_{eff}}$$

a) $CL_{metab} + CL_{seq} >> CL_{eff}$

$$CLu_{int} \sim CL_{inf} \quad \text{(uptake-limited)}$$

b) $CL_{metab} + CL_{seq} << CL_{eff}$

$$CLu_{int} = CL_{inf} \times \frac{CL_{metab} + CL_{seq}}{CL_{eff}}$$

3) The effect of the change in apparent intrinsic clearance on the hepatic clearance of drugs

Assuming that drug is eliminated only from liver...

$$AUC_h = \frac{Dose}{CL_{hep}}$$

$$CL_{hep} = \frac{Q_h \times f_B CLu_{int}}{Q_h + f_B CLu_{int}}$$

i.v. administration

Blood-flow limited

$$AUC_h \sim \frac{Dose}{Q_h}$$

Intrinsic clearance limited

$$AUC_h \sim \frac{Dose}{f_B CLu_{int}}$$

p.o. administration

$$AUC_h \sim \frac{Fh \times Dose}{CL_{hep}} = \frac{Dose}{f_B CLu_{int}}$$

Fig. C-1 The key factors for the determination of pharmacokinetics of drugs

References

Abe T, Kakyo M, Tokui T, Nakagomi R, Nishio T, Nakai D, Nomura H, Unno M, Suzuki M, Naitoh T, Matsuno S and Yawo H (1999) Identification of a novel gene family encoding human liver-specific organic anion transporter LST-1. *J Biol Chem* **274**:17159-17163.

Alcorn J, Lu X, Moscow JA and McNamara PJ (2002) Transporter gene expression in lactating and nonlactating human mammary epithelial cells using real-time reverse transcription-polymerase chain reaction. *J Pharmacol Exp Ther* **303**:487-496.

Anwer MS and Hegner D (1978) Effect of Na on bile acid uptake by isolated rat hepatocytes. Evidence for a heterogeneous system. *Hoppe Seylers Z Physiol Chem* **359**:181-192.

Bi YA, Kazolias DC and Duignan DB (2006) Use of Cryopreserved Human Hepatocytes in Sandwich-Culture to Measure Hepatobiliary Transport. *Drug Metab Dispos.*

Bouscarel B, Nussbaum R, Dubner H and Fromm H (1995) The role of sodium in the uptake of ursodeoxycholic acid in isolated hamster hepatocytes. *Hepatology* **21**:145-154.

Briz O, Serrano MA, Rebollo N, Hagenbuch B, Meier PJ, Koepsell H and Marin JJ (2002) Carriers involved in targeting the cytostatic bile acid-cisplatin derivatives cis-diammine-chloro-cholylglycinate-platinum(II) and cis-diammine-bisursodeoxycholate-platinum(II) toward liver cells. *Mol Pharmacol* **61**:853-860.

Byrne JA, Strautnieks SS, Mieli-Vergani G, Higgins CF, Linton KJ and Thompson RJ (2002) The human bile salt export pump: characterization of substrate specificity and identification of inhibitors. *Gastroenterology* **123**:1649-1658.

Chung JY, Cho JY, Yu KS, Kim JR, Oh DS, Jung HR, Lim KS, Moon KH, Shin SG and Jang IJ (2005) Effect of OATP1B1 (SLCO1B1) variant alleles on the pharmacokinetics of pitavastatin in healthy volunteers. *Clin Pharmacol Ther* **78**:342-350.

Criscione L, Bradley W, Buhlmayer P, Whitebread S, Glazer R, Lloyd P, Mueller P and de Gasparo M (1995) Valsartan: pre-clinical and clinical profile of an anthypertensive angiotensin-II antagonist. *Cardiovasc Drug Rev* **13**:230-250.

Crosignani A, Setchell KD, Invernizzi P, Larghi A, Rodrigues CM and Podda M

(1996) Clinical pharmacokinetics of therapeutic bile acids. *Clin Pharmacokinet* **30**:333-358.

Cui Y, Konig J, Leier I, Buchholz U and Keppler D (2001) Hepatic uptake of bilirubin and its conjugates by the human organic anion transporter SLC21A6. *J Biol Chem* **276**:9626-9630.

Dietrich CG, de Waart DR, Ottenhoff R, Schoots IG and Elferink RP (2001) Increased bioavailability of the food-derived carcinogen 2-amino-1-methyl-6-phenylimidazo[4,5-b]pyridine in MRP2-deficient rats. *Mol Pharmacol* **59**:974-980.

Eckhardt U, Schroeder A, Stieger B, Hochli M, Landmann L, Tynes R, Meier PJ and Hagenbuch B (1999) Polyspecific substrate uptake by the hepatic organic anion transporter Oatp1 in stably transfected CHO cells. *Am J Physiol* **276**:G1037-1042.

Ewerth S, Angelin B, Einarsson K, Nilsell K and Bjorkhem I (1985) Serum concentrations of ursodeoxycholic acid in portal venous and systemic venous blood of fasting humans as determined by isotope dilution-mass spectrometry. *Gastroenterology* **88**:126-133.

Hagenbuch B and Meier PJ (1994) Molecular cloning, chromosomal localization,

and functional characterization of a human liver Na+/bile acid cotransporter. *J Clin Invest* **93**:1326-1331.

Hagenbuch B and Meier PJ (1996) Sinusoidal (basolateral) bile salt uptake systems of hepatocytes. *Semin Liver Dis* **16**:129-136.

Hagenbuch B and Meier PJ (2003) The superfamily of organic anion transporting polypeptides. *Biochim Biophys Acta* **1609**:1-18.

Hata S, Wang P, Eftychiou N, Ananthanarayanan M, Batta A, Salen G, Pang KS and Wolkoff AW (2003) Substrate specificities of rat oatp1 and ntcp: implications for hepatic organic anion uptake. *Am J Physiol Gastrointest Liver Physiol* **285**:G829-839.

Hengstler JG, Utesch D, Steinberg P, Platt KL, Diener B, Ringel M, Swales N, Fischer T, Biefang K, Gerl M, Bottger T and Oesch F (2000) Cryopreserved primary hepatocytes as a constantly available in vitro model for the evaluation of human and animal drug metabolism and enzyme induction. *Drug Metab Rev* **32**:81-118.

Hirano M, Maeda K, Shitara Y and Sugiyama Y (2004) Contribution of OATP2 (OATP1B1) and OATP8 (OATP1B3) to the hepatic uptake of pitavastatin in humans. *J Pharmacol Exp Ther* **311**:139-146.

Hirano M, Maeda K, Shitara Y and Sugiyama Y (2006) Drug-drug interaction between pitavastatin and various drugs via OATP1B1. *Drug Metab Dispos* **34**:1229-1236.

Hoffmaster KA, Turncliff RZ, LeCluyse EL, Kim RB, Meier PJ and Brouwer KL (2004) P-glycoprotein expression, localization, and function in sandwich-cultured primary rat and human hepatocytes: relevance to the hepatobiliary disposition of a model opioid peptide. *Pharm Res* **21**:1294-1302.

Hofmann AF (1999) The continuing importance of bile acids in liver and intestinal disease. *Arch Intern Med* **159**:2647-2658.

Hsiang B, Zhu Y, Wang Z, Wu Y, Sasseville V, Yang WP and Kirchgessner TG (1999) A novel human hepatic organic anion transporting polypeptide (OATP2). Identification of a liver-specific human organic anion transporting polypeptide and identification of rat and human hydroxymethylglutaryl-CoA reductase inhibitor transporters. *J Biol Chem* **274**:37161-37168.

Igel M, Arnold KA, Niemi M, Hofmann U, Schwab M, Lutjohann D, von Bergmann K, Eichelbaum M and Kivisto KT (2006) Impact of the

SLCO1B1 polymorphism on the pharmacokinetics and lipid-lowering efficacy of multiple-dose pravastatin. *Clin Pharmacol Ther* **79**:419-426.

Invernizzi P, Setchell KD, Crosignani A, Battezzati PM, Larghi A, O'Connell NC and Podda M (1999) Differences in the metabolism and disposition of ursodeoxycholic acid and of its taurine-conjugated species in patients with primary biliary cirrhosis. *Hepatology* **29**:320-327.

Ishigami M, Tokui T, Komai T, Tsukahara K, Yamazaki M and Sugiyama Y (1995) Evaluation of the uptake of pravastatin by perfused rat liver and primary cultured rat hepatocytes. *Pharm Res* **12**:1741-1745.

Ishiguro N, Maeda K, Kishimoto W, Saito A, Harada A, Ebner T, Roth W, Igarashi T and Sugiyama Y (2006) Predominant contribution of OATP1B3 to the hepatic uptake of telmisartan, an angiotensin II receptor antagonist, in humans. *Drug Metab Dispos* **34**:1109-1115.

Ishii T, Yasuchika K, Fujii H, Hoppo T, Baba S, Naito M, Machimoto T, Kamo N, Suemori H, Nakatsuji N and Ikai I (2005) In vitro differentiation and maturation of mouse embryonic stem cells into hepatocytes. *Exp Cell Res* **309**:68-77.

Ishizuka H, Konno K, Naganuma H, Sasahara K, Kawahara Y, Niinuma K,

Suzuki H and Sugiyama Y (1997) Temocaprilat, a novel angiotensin-converting enzyme inhibitor, is excreted in bile via an ATP-dependent active transporter (cMOAT) that is deficient in Eisai hyperbilirubinemic mutant rats (EHBR). *J Pharmacol Exp Ther* **280**:1304-1311.

Israili ZH (2000) Clinical pharmacokinetics of angiotensin II (AT1) receptor blockers in hypertension. *J Hum Hypertens* **14 Suppl 1**:S73-86.

Iwai M, Suzuki H, Ieiri I, Otsubo K and Sugiyama Y (2004) Functional analysis of single nucleotide polymorphisms of hepatic organic anion transporter OATP1B1 (OATP-C). *Pharmacogenetics* **14**:749-757.

Kameyama Y, Yamashita K, Kobayashi K, Hosokawa M and Chiba K (2005) Functional characterization of SLCO1B1 (OATP-C) variants, SLCO1B1*5, SLCO1B1*15 and SLCO1B1*15+C1007G, by using transient expression systems of HeLa and HEK293 cells. *Pharmacogenet Genomics* **15**:513-522.

Katz DA, Carr R, Grimm DR, Xiong H, Holley-Shanks R, Mueller T, Leake B, Wang Q, Han L, Wang PG, Edeki T, Sahelijo L, Doan T, Allen A, Spear BB and Kim RB (2006) Organic anion transporting polypeptide 1B1 activity

classified by SLCO1B1 genotype influences atrasentan pharmacokinetics. *Clin Pharmacol Ther* **79**:186-196.

Kawabata K, Samata N and Urasaki Y (2005) Quantitative determination of pravastatin and R-416, its main metabolite in human plasma, by liquid chromatography-tandem mass spectrometry. *J Chromatogr B Analyt Technol Biomed Life Sci* **816**:73-79.

Kim RB, Leake B, Cvetkovic M, Roden MM, Nadeau J, Walubo A and Wilkinson GR (1999) Modulation by drugs of human hepatic sodium-dependent bile acid transporter (sodium taurocholate cotransporting polypeptide) activity. *J Pharmacol Exp Ther* **291**:1204-1209.

Konig J, Cui Y, Nies AT and Keppler D (2000) A novel human organic anion transporting polypeptide localized to the basolateral hepatocyte membrane. *Am J Physiol Gastrointest Liver Physiol* **278**:G156-164.

Konig J, Nies AT, Cui Y, Leier I and Keppler D (1999) Conjugate export pumps of the multidrug resistance protein (MRP) family: localization, substrate specificity, and MRP2-mediated drug resistance. *Biochim Biophys Acta* **1461**:377-394.

Kullak-Ublick GA, Hagenbuch B, Stieger B, Schteingart CD, Hofmann AF,

Wolkoff AW and Meier PJ (1995) Molecular and functional characterization of an organic anion transporting polypeptide cloned from human liver. *Gastroenterology* **109**:1274-1282.

Lee E, Ryan S, Birmingham B, Zalikowski J, March R, Ambrose H, Moore R, Lee C, Chen Y and Schneck D (2005) Rosuvastatin pharmacokinetics and pharmacogenetics in white and Asian subjects residing in the same environment. *Clin Pharmacol Ther* **78**:330-341.

Lee YJ, Maeda J, Kusuhara H, Okauchi T, Inaji M, Nagai Y, Obayashi S, Nakao R, Suzuki K, Sugiyama Y and Suhara T (2006) In vivo evaluation of P-glycoprotein function at the blood-brain barrier in nonhuman primates using [11C]verapamil. *J Pharmacol Exp Ther* **316**:647-653.

Levin VA (1980) Relationship of octanol/water partition coefficient and molecular weight to rat brain capillary permeability. *J Med Chem* **23**:682-684.

Lindor KD, Lacerda MA, Jorgensen RA, DeSotel CK, Batta AK, Salen G, Dickson ER, Rossi SS and Hofmann AF (1998) Relationship between biliary and serum bile acids and response to ursodeoxycholic acid in patients with primary biliary cirrhosis. *Am J Gastroenterol* **93**:1498-1504.

Matsushima S, Maeda K, Kondo C, Hirano M, Sasaki M, Suzuki H and

Sugiyama Y (2005) Identification of the hepatic efflux transporters of organic anions using double-transfected Madin-Darby canine kidney II cells expressing human organic anion-transporting polypeptide 1B1 (OATP1B1)/multidrug resistance-associated protein 2, OATP1B1/multidrug resistance 1, and OATP1B1/breast cancer resistance protein. *J Pharmacol Exp Ther* **314**:1059-1067.

Meier PJ, Eckhardt U, Schroeder A, Hagenbuch B and Stieger B (1997) Substrate specificity of sinusoidal bile acid and organic anion uptake systems in rat and human liver. *Hepatology* **26**:1667-1677.

Mizuno N, Niwa T, Yotsumoto Y and Sugiyama Y (2003) Impact of drug transporter studies on drug discovery and development. *Pharmacol Rev* **55**:425-461.

Muller M and Jansen PL (1997) Molecular aspects of hepatobiliary transport. *Am J Physiol* **272**:G1285-1303.

Mwinyi J, Johne A, Bauer S, Roots I and Gerloff T (2004) Evidence for inverse effects of OATP-C (SLC21A6) 5 and 1b haplotypes on pravastatin kinetics. *Clin Pharmacol Ther* **75**:415-421.

Nakai D, Nakagomi R, Furuta Y, Tokui T, Abe T, Ikeda T and Nishimura K (2001)

Human liver-specific organic anion transporter, LST-1, mediates uptake of pravastatin by human hepatocytes. *J Pharmacol Exp Ther* **297**:861-867.

Niemi M, Backman JT, Kajosaari LI, Leathart JB, Neuvonen M, Daly AK, Eichelbaum M, Kivisto KT and Neuvonen PJ (2005a) Polymorphic organic anion transporting polypeptide 1B1 is a major determinant of repaglinide pharmacokinetics. *Clin Pharmacol Ther* **77**:468-478.

Niemi M, Kivisto KT, Hofmann U, Schwab M, Eichelbaum M and Fromm MF (2005b) Fexofenadine pharmacokinetics are associated with a polymorphism of the SLCO1B1 gene (encoding OATP1B1). *Br J Clin Pharmacol* **59**:602-604.

Niemi M, Neuvonen PJ, Hofmann U, Backman JT, Schwab M, Lutjohann D, von Bergmann K, Eichelbaum M and Kivisto KT (2005c) Acute effects of pravastatin on cholesterol synthesis are associated with SLCO1B1 (encoding OATP1B1) haplotype *17. *Pharmacogenet Genomics* **15**:303-309.

Niemi M, Schaeffeler E, Lang T, Fromm MF, Neuvonen M, Kyrklund C, Backman JT, Kerb R, Schwab M, Neuvonen PJ, Eichelbaum M and Kivisto KT (2004) High plasma pravastatin concentrations are associated with single

nucleotide polymorphisms and haplotypes of organic anion transporting polypeptide-C (OATP-C, SLCO1B1). *Pharmacogenetics* **14**:429-440.

Nishizato Y, Ieiri I, Suzuki H, Kimura M, Kawabata K, Hirota T, Takane H, Irie S, Kusuhara H, Urasaki Y, Urae A, Higuchi S, Otsubo K and Sugiyama Y (2003) Polymorphisms of OATP-C (SLC21A6) and OAT3 (SLC22A8) genes: consequences for pravastatin pharmacokinetics. *Clin Pharmacol Ther* **73**:554-565.

Noe J, Hagenbuch B, Meier PJ and St-Pierre MV (2001) Characterization of the mouse bile salt export pump overexpressed in the baculovirus system. *Hepatology* **33**:1223-1231.

Noe J, Stieger B and Meier PJ (2002) Functional expression of the canalicular bile salt export pump of human liver. *Gastroenterology* **123**:1659-1666.

Nozawa T, Imai K, Nezu J, Tsuji A and Tamai I (2004) Functional characterization of pH-sensitive organic anion transporting polypeptide OATP-B in human. *J Pharmacol Exp Ther* **308**:438-445.

Nozawa T, Minami H, Sugiura S, Tsuji A and Tamai I (2005) Role of organic anion transporter OATP1B1 (OATP-C) in hepatic uptake of irinotecan and its active metabolite, 7-ethyl-10-hydroxycamptothecin: in vitro evidence

and effect of single nucleotide polymorphisms. *Drug Metab Dispos* **33**:434-439.

Ogawa K, Suzuki H, Hirohashi T, Ishikawa T, Meier PJ, Hirose K, Akizawa T, Yoshioka M and Sugiyama Y (2000) Characterization of inducible nature of MRP3 in rat liver. *Am J Physiol Gastrointest Liver Physiol* **278**:G438-446.

Oizumi K, Koike H, Sada T, Miyamoto M, Nishino H, Matsushita Y, Iijima Y and Yanagisawa H (1988) Pharmacological profiles of CS-622, a novel angiotensin converting enzyme inhibitor. *Jpn J Pharmacol* **48**:349-356.

Paumgartner G and Beuers U (2002) Ursodeoxycholic acid in cholestatic liver disease: mechanisms of action and therapeutic use revisited. *Hepatology* **36**:525-531.

Poupon R, Chretien Y, Parquet M, Ballet F, Rey C and Infante R (1988) Hepatic transport of bile acids in the isolated perfused rat liver. Structure-kinetic relationship. *Biochem Pharmacol* **37**:209-212.

Reichel C, Gao B, Van Montfoort J, Cattori V, Rahner C, Hagenbuch B, Stieger B, Kamisako T and Meier PJ (1999) Localization and function of the organic anion-transporting polypeptide Oatp2 in rat liver. *Gastroenterology*

117:688-695.

Rippin SJ, Hagenbuch B, Meier PJ and Stieger B (2001) Cholestatic expression pattern of sinusoidal and canalicular organic anion transport systems in primary cultured rat hepatocytes. *Hepatology* **33**:776-782.

Sasaki M, Suzuki H, Aoki J, Ito K, Meier PJ and Sugiyama Y (2004) Prediction of in vivo biliary clearance from the in vitro transcellular transport of organic anions across a double-transfected Madin-Darby canine kidney II monolayer expressing both rat organic anion transporting polypeptide 4 and multidrug resistance associated protein 2. *Mol Pharmacol* **66**:450-459.

Sasaki M, Suzuki H, Ito K, Abe T and Sugiyama Y (2002) Transcellular transport of organic anions across a double-transfected Madin-Darby canine kidney II cell monolayer expressing both human organic anion-transporting polypeptide (OATP2/SLC21A6) and Multidrug resistance-associated protein 2 (MRP2/ABCC2). *J Biol Chem* **277**:6497-6503.

Sasongko L, Link JM, Muzi M, Mankoff DA, Yang X, Collier AC, Shoner SC and Unadkat JD (2005) Imaging P-glycoprotein transport activity at the human blood-brain barrier with positron emission tomography. *Clin Pharmacol*

Ther **77**:503-514.

Schmidt EK, Antonin KH, Flesch G and Racine-Poon A (1998) An interaction study with cimetidine and the new angiotensin II antagonist valsartan. *Eur J Clin Pharmacol* **53**:451-458.

Schroeder A, Eckhardt U, Stieger B, Tynes R, Schteingart CD, Hofmann AF, Meier PJ and Hagenbuch B (1998) Substrate specificity of the rat liver Na(+)-bile salt cotransporter in Xenopus laevis oocytes and in CHO cells. *Am J Physiol* **274**:G370-375.

Shimizu M, Fuse K, Okudaira K, Nishigaki R, Maeda K, Kusuhara H and Sugiyama Y (2005) Contribution of OATP (organic anion-transporting polypeptide) family transporters to the hepatic uptake of fexofenadine in humans. *Drug Metab Dispos* **33**:1477-1481.

Shitara Y, Itoh T, Sato H, Li AP and Sugiyama Y (2003a) Inhibition of transporter-mediated hepatic uptake as a mechanism for drug-drug interaction between cerivastatin and cyclosporin A. *J Pharmacol Exp Ther* **304**:610-616.

Shitara Y, Li AP, Kato Y, Lu C, Ito K, Itoh T and Sugiyama Y (2003b) Function of uptake transporters for taurocholate and estradiol 17beta-D-glucuronide

in cryopreserved human hepatocytes. *Drug Metab Pharmacokinet* **18**:33-41.

Shitara Y, Sato H and Sugiyama Y (2005) Evaluation of drug-drug interaction in the hepatobiliary and renal transport of drugs. *Annu Rev Pharmacol Toxicol* **45**:689-723.

Singhvi SM, Pan HY, Morrison RA and Willard DA (1990) Disposition of pravastatin sodium, a tissue-selective HMG-CoA reductase inhibitor, in healthy subjects. *Br J Clin Pharmacol* **29**:239-243.

Sorscher S, Lillienau J, Meinkoth JL, Steinbach JH, Schteingart CD, Feramisco J and Hofmann AF (1992) Conjugated bile acid uptake by Xenopus laevis oocytes induced by microinjection with ileal Poly A+ mRNA. *Biochem Biophys Res Commun* **186**:1455-1462.

Sun W, Wu RR, van Poelje PD and Erion MD (2001) Isolation of a family of organic anion transporters from human liver and kidney. *Biochem Biophys Res Commun* **283**:417-422.

Suzuki H and Sugiyama Y (1998) Excretion of GSSG and glutathione conjugates mediated by MRP1 and cMOAT/MRP2. *Semin Liver Dis* **18**:359-376.

Suzuki M, Suzuki H, Sugimoto Y and Sugiyama Y (2003) ABCG2 transports

sulfated conjugates of steroids and xenobiotics. *J Biol Chem* **278**:22644-22649.

Tachibana-Iimori R, Tabara Y, Kusuhara H, Kohara K, Kawamoto R, Nakura J, Tokunaga K, Kondo I, Sugiyama Y and Miki T (2004) Effect of genetic polymorphism of OATP-C (SLCO1B1) on lipid-lowering response to HMG-CoA reductase inhibitors. *Drug Metab Pharmacokinet* **19**:375-380.

Takikawa H, Takemura T and Yamanaka M (1995) The mechanism of tauroursodeoxycholate uptake by isolated rat hepatocytes. *Int Hepatol Commun* **3**:20-25.

Tamai I, Takanaga H, Maeda H, Ogihara T, Yoneda M and Tsuji A (1995) Proton-cotransport of pravastatin across intestinal brush-border membrane. *Pharm Res* **12**:1727-1732.

Tanaka E, Kurata N and Yasuhara H (2003) How useful is the "cocktail approach" for evaluating human hepatic drug metabolizing capacity using cytochrome P450 phenotyping probes in vivo? *J Clin Pharm Ther* **28**:157-165.

Tanigawara Y (2000) Role of P-glycoprotein in drug disposition. *Ther Drug Monit* **22**:137-140.

Tian X, Zamek-Gliszczynski MJ, Zhang P and Brouwer KL (2004) Modulation of multidrug resistance-associated protein 2 (Mrp2) and Mrp3 expression and function with small interfering RNA in sandwich-cultured rat hepatocytes. *Mol Pharmacol* **66**:1004-1010.

Tirona RG, Leake BF, Merino G and Kim RB (2001) Polymorphisms in OATP-C: identification of multiple allelic variants associated with altered transport activity among European- and African-Americans. *J Biol Chem* **276**:35669-35675.

Triscari J, O'Donnell D, Zinny M and Pan HY (1995) Gastrointestinal absorption of pravastatin in healthy subjects. *J Clin Pharmacol* **35**:142-144.

Van Dyke RW, Stephens JE and Scharschmidt BF (1982) Bile acid transport in cultured rat hepatocytes. *Am J Physiol* **243**:G484-492.

van Herwaarden AE, Jonker JW, Wagenaar E, Brinkhuis RF, Schellens JH, Beijnen JH and Schinkel AH (2003) The breast cancer resistance protein (Bcrp1/Abcg2) restricts exposure to the dietary carcinogen 2-amino-1-methyl-6-phenylimidazo[4,5-b]pyridine. *Cancer Res* **63**:6447-6452.

Varadi A, Szakacs G, Bakos E and Sarkadi B (2002) P glycoprotein and the

mechanism of multidrug resistance. *Novartis Found Symp* **243**:54-65; discussion 65-58, 180-185.

von Dippe P, Amoui M, Stellwagen RH and Levy D (1996) The functional expression of sodium-dependent bile acid transport in Madin-Darby canine kidney cells transfected with the cDNA for microsomal epoxide hydrolase. *J Biol Chem* **271**:18176-18180.

Waldmeier F, Flesch G, Muller P, Winkler T, Kriemler HP, Buhlmayer P and De Gasparo M (1997) Pharmacokinetics, disposition and biotransformation of [14C]-radiolabelled valsartan in healthy male volunteers after a single oral dose. *Xenobiotica* **27**:59-71.

Walters HC, Craddock AL, Fusegawa H, Willingham MC and Dawson PA (2000) Expression, transport properties, and chromosomal location of organic anion transporter subtype 3. *Am J Physiol Gastrointest Liver Physiol* **279**:G1188-1200.

Yamaoka K, Tanigawara Y, Nakagawa T and Uno T (1981) A pharmacokinetic analysis program (multi) for microcomputer. *J Pharmacobiodyn* **4**:879-885.

Yamashiro W, Maeda K, Hirouchi M, Adachi Y, Hu Z and Sugiyama Y (2006)

Involvement of transporters in the hepatic uptake and biliary excretion of valsartan, a selective antagonist of the angiotensin II AT1-receptor, in humans. *Drug Metab Dispos* **34**:1247-1254.

Yamazaki M, Suzuki H and Sugiyama Y (1996) Recent advances in carrier-mediated hepatic uptake and biliary excretion of xenobiotics. *Pharm Res* **13**:497-513.

Zhang L, Dresser MJ, Gray AT, Yost SC, Terashita S and Giacomini KM (1997) Cloning and functional expression of a human liver organic cation transporter. *Mol Pharmacol* **51**:913-921.

Zhang W, He YJ, Han CT, Liu ZQ, Li Q, Fan L, Tan ZR, Zhang WX, Yu BN, Wang D, Hu DL and Zhou HH (2006a) Effect of SLCO1B1 genetic polymorphism on the pharmacokinetics of nateglinide. *Br J Clin Pharmacol*.

Zhang W, Yu BN, He YJ, Fan L, Li Q, Liu ZQ, Wang A, Liu YL, Tan ZR, Fen J, Huang YF and Zhou HH (2006b) Role of BCRP 421C>A polymorphism on rosuvastatin pharmacokinetics in healthy Chinese males. *Clin Chim Acta*.

Zuber R, Anzenbacherova E and Anzenbacher P (2002) Cytochromes P450 and experimental models of drug metabolism. *J Cell Mol Med* **6**:189-198.

Acknowledgements

I would like to express my sincere appreciation to Prof. Yuichi Sugiyama for his kind and meticulous teaching and valuable discussions throughout the entire period of my research. I also want to thank Dr. Hiroyuki Kusuhara (Assoc. Prof.) and Dr. Reiko Onuki (Assist. Prof.) for their fruitful discussion and continuous encouragement for my study. I am also grateful to Dr. Yukio Kato (Assoc. Prof. in Kanazawa Univ.; the former supervisor in my master-course) and Dr. Hiroshi Suzuki (Prof. in Tokyo University Hospital; the former Assoc. Prof. in our Lab.) for their intensive education and helpful suggestions.

In Part I, I want to express my great thanks to Prof. Alan F. Hofmann (Department of Medicine, University of California, San Diego) for kindly providing radiolabeled bile acids and giving me valuable discussion. I also thank Mitsubishi Pharma Co. for supplying unlabeled UDCA, TUDC and GUDC. I am also grateful to Ms. Miyuki Kambara and Ms. Ying Tian for supporting my experiments.

In Part II, I would like to express my deepest thanks to Prof. Ichiro Ieiri (Kyushu Univ.) for his kind support and valuable discussion. I am also grateful to Dr. Hiroaki Fujiwara and Dr. Akiharu Fujino in Fuji Biomedix Co. Ltd. and Dr.

Kuninobu Yasuda in Kannondai-Clinic for their kind and intensive support of our clinical study. I also want to thank Mr. Masaru Hirano, Mr. Takao Watanabe and Mr. Yoshiaki Kitamura for their kind support of *in vitro* study. I would like to thank Sankyo Co., Ltd. for providing us with Mevalotin tablets, Acecol tablets, [^{14}C]-labeled and unlabeled temocaprilat, temocapril, RMS-416 and R-122798, and Novartis Pharma K.K. for providing us with Diovan tablets and [^{3}H]-labeled and unlabeled valsartan. I am also grateful to Dr. Kiyoshi Kawabata (Sankyo Co., Ltd.) for teaching us the method for the quantification of pravastatin, RMS-416, temocapril and temocaprilat. I am also grateful to Dr. Ryosei Kawai and Dr. Yuko Tsukamoto (Novartis Pharma K.K.), and Dr. Toshihiko Ikeda, Dr. Yasushi Orihashi, and Dr. Hideo Naganuma (Sankyo Co., Ltd.) for supporting our study and giving me helpful suggestions.

I would like to express my sincere thanks to all of the members in the Department of Molecular Pharmacokinetics for their kind support and encouragement.

Finally, I appreciate my father and mother so much for their continuous encouragement.